THESIS FOR THE DEGREE OF DOCTOR OF PHILOSOPHY

Exploring new protic ionic liquids

From synthesis to fundamental properties

Eduardo Maurina Morais

Department of Chemistry and Chemical Engineering
CHALMERS UNIVERSITY OF TECHNOLOGY
Gothenburg, Sweden 2023

Exploring new protic ionic liquids

From synthesis to fundamental properties

Eduardo Maurina Morais

ISBN 978-91-7905-960-6

Doktorsavhandlingar vid Chalmers tekniska högskola

Ny serie Nr. 5426

ISSN 0346-718X

Department of Chemistry and Chemical Engineering
Chalmers University of Technology
SE-412 96 Gothenburg
Telephone +46 31 772 1000

Cover:
A chemist exploring a sky of possibilities

Typeset in LaTeX using the kaobook class
Printed by Chalmers Digitaltryck
Gothenburg, Sweden 2023

Exploring new protic ionic liquids
From synthesis to fundamental properties
Eduardo Maurina Morais
Department of Chemistry and Chemical Engineering
Chalmers University of Technology

Abstract

The ionic liquid community frequently leverages the selling point that more than a million new ionic liquids could conceivably be created. Nonetheless, the number of commercially available compounds is orders of magnitude lower. This highlights the fact that only a small number of all possible ionic liquids are actively being researched, a reality particularly noticeable in the niche field of protic ionic liquids. In such a scenario, research focusing on the development of even a small number of viable alternatives to the popular alkylammonium- and imidazolium-based cations could potentially have a big impact, by paving the way for the synthesis of new families of ionic liquids. However, for these new alternatives to be widely used by the community, they must be easy to synthesize and have desirable properties.

In this thesis, I discuss the challenges that I have encountered and the lessons that I have learned while trying to explore the chemical space of protic ionic liquids. This exploration started with the development of a procedure for the synthesis of pure and dry protic ionic liquids, which was used to make new triazolium-based protic ionic liquids. Additionally, this first work highlights the importance of using air-free techniques to analyze these hygroscopic compounds. Later, these insights were used to develop a new setup for the determination of ionic conductivity in ionic liquids. The latter was used in conjunction with pulsed-field gradient nuclear magnetic resonance diffusion experiments and density functional theory experiments to understand the differences in transport properties between triazolium- and imidazolium-based protic ionic liquids. Finally, we once again turned our attention to the imidazolium cation and explored how simple modifications to its electronic structure, by means of functionalization with electron-withdrawing groups, can enhance its acidity, and how that affects the properties of these nitro- and cyano-functionalized protic ionic liquids.

This thesis aims to highlight the importance of developing new methods for the synthesis and analysis of protic ionic liquids, as well as to explore how computational modeling can be used to rationalize the observed differences in the physicochemical properties of these compounds.

Keywords: Protic ionic liquids, acidity, transport properties, thermal analysis, DFT

List of Publications

This thesis is based on the following appended papers, referred to by Roman numerals in the text:

I. Solvent-free synthesis of protic ionic liquids. Synthesis, characterization and computational studies of triazolium based ionic liquids

E. M. Morais , I. Abdurrokhman, and A. Martinelli

Journal of Molecular Liquids, 360 **(2022)**, 119358

II. Transport properties of protic ionic liquids based on triazolium and imidazolium: Development of an air-free conductivity setup

E. M. Morais , A. Idström, L. Evenäs and A. Martinelli

Molecules, 28 **(2023)**, 5147

III. Enhancing the acidity of imidazolium protic ionic liquids by nitro- and cyano-functionalization

E. Dahlqvist, E. M. Morais and A. Martinelli

Submitted to the Journal of Ionic Liquids **(August 2023)**

My contribution to the publications

Paper I

Shared first author. Idealized and designed the protic ionic liquid reaction setup and synthetic strategies, as well as the air-free techniques for analysis. Performed all experiments with the shared first author. Performed all the computational experiments and evaluated the results. Both first authors processed the experimental data, performed the analysis, and drafted the manuscript. Was the main responsible for the submission process and the revision process after peer review.

Paper II

Designed the glovebox conductivity setup. Designed and performed all experiments, with the exception of the pulsed-field gradient NMR spectroscopy measurements. Performed all the computational experiments and evaluated the results. Together with Anna Martinelli, we processed the experimental data, performed the analysis, and drafted the manuscript, with the exception of the pulsed-field gradient NMR spectroscopy method description and data processing, which was handled by Alexander Idström and Lars Evenäs. Was the main responsible for the submission process and the revision process after peer review.

Paper III

Idealized the concept and synthetic strategies. Designed and performed all experiments with the shared first author. Supervised the shared first author. Performed all the computational experiments and evaluated the results. Together with Eva Dahlqvist, we processed the experimental data, performed the analysis, and drafted the manuscript. Was the main responsible for the submission process.

Acknowledgements

I did not do it alone. I didn't come this far because I'm special, I did it because others helped me. They pushed me forward, they truly helped me. It might sound weird coming from someone who just did a PhD, but during high school, I didn't like studying at all. Nowadays, I love it! All because I had a little help from a high school chemistry teacher, Prof. Denise K. da Costa. I was also lucky to have professors who inspired me during my Bachelor's. The opportunities they gave me were invaluable. So thank you, Prof. Andre Arigony, Prof. Sandra Einlof, and Prof. Marcus Seferin. During my Master's, under the guidance of Prof. Jackson D. Scholten, I became a better scientist. And during the PhD, Prof. Anna Martinelli pushed me to go even further. Anna, you are an incredibly smart, caring, and hardworking scientist. I wouldn't have made it if it wasn't for your constant support. Thank you for giving me this amazing opportunity.

I also thank my co-supervisor Prof. Itai Panas for the inspiring conversations and my examiner Prof. Magnus Skoglundh for all the time and effort to get me this far. Finally, I want to acknowledge my collaborators Prof. Lars Evenäs and Dr. Alexander Idström for their excellent work on Paper II, and all the partners in the HIONIC project.

Funding from the Swedish Research Council, the Swedish Energy Agency, and the Knut and Alice Wallenberg Foundation is kindly acknowledged, as well as support from the Swedish NMR Centre and Swedish National Infrastructure for Computing.

Although I loved the entire PhD journey, it was not easy. But amazing people around me helped me through it. My colleagues at the Division of Applied Chemistry made my days at work fun and relaxed, thank you for all the parties and fikas. Special thanks to all members of the Martinelli group, Eva, Giannis, Iqbaal, Khalid, Mohammad, Nicole, Olesia, Szilvia, and Vandna.

Outside of work, my climbing friends helped me relax. They took me to some of the most beautiful places I've ever seen and pushed me to do stuff I didn't even think I was capable of. Thank you so much. Snail boys forever!

The endless support that my family back in Brazil provided during these last few years is beyond words (but I'll give it a try in Portuguese anyways). Mãe, como tu bem sabe, eu não sou muito bom com palavras, então vou ser curto e grosso! Eu te amo muito! Obrigado por sempre acreditar em mim e por ter sempre lutado muito para me dar uma excelente educação.

The last two people I wanna thank should be getting a PhD as well, for the amount of work and stress I put them through. Thank you, Abril and Fabi.

Eduardo Maurina Morais, Gothenburg, December 2023

Contents

List of Figures

List of Tables

Introduction 1

When I first started thinking about the title of this thesis, the first term that came to my mind was "to explore". Simply out of curiosity, I decided to ask the artificial intelligence model ChatGPT what is the meaning of this word, to which it replied: "To explore refers to the act of investigating, discovering, or examining something, often with the goal of gaining knowledge, understanding, or experience. It typically involves venturing into new or unfamiliar territories, whether they are physical, intellectual, or conceptual", which is quite a decent definition of what my PhD work felt like. Exploration also seems to imply a non-linear journey, with twists and turns, with a fairly well-defined starting point, but a blurry endpoint. The starting point of this exploration was the development of new proton-conducting materials for intermediate temperature proton exchange membrane fuel cells[1] and, although I don't believe that this journey has reached a final destination yet, it has led me to a better understanding of the fundamental properties of protic ionic liquids, especially in regards to how these properties are influenced by acidity. In this thesis, I will discuss the challenges involved in this endeavor, from how to make new compounds, how to analyze them, and how to use computational tools to better understand them.

1: So-called high temperature PEM fuel cells (HT-PEMFC) are expected to operate at temperatures between 120 to 200 °C since they don't use water as the proton-conducting medium.

1.1 What are protic ionic liquids?

In short, protic ionic liquids are low melting point salts[2] formed by the reaction between a Brønsted acid and a Brønsted base [1] (Figure 1.1). They belong to the broader class of ionic liquids, which are mostly represented by aprotic ionic liquids, i.e. analogous compounds commonly formed by quaternization reactions of amines with alkyl halides (Figure 1.1).

2: Ionic liquids are typically defined as having melting points below 100 °C; however, this is an arbitrary definition that is employed with some flexibility, meaning that some compounds with melting points exceeding 100 °C are still categorized as ionic liquids, as long as they share other characteristics with this class of compounds.

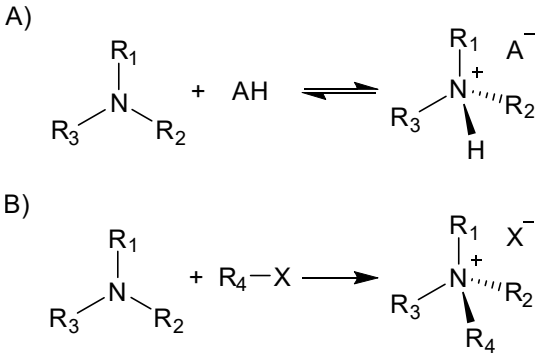

Figure 1.1: Generic reaction schemes for the synthesis of protic (A) and aprotic (B) ionic liquids. Note that most aprotic ionic liquid syntheses still require a subsequent salt metathesis reaction to substitute the halogen anion for another more suitable anion.

Although aprotic ionic liquids are significantly more commonly addressed in the literature, the first widely recognized report of a room-temperature ionic liquid[3] was published in 1914 by Paul Walden [2], which described the discovery of the protic ionic liquid ethylammonium nitrate. Curiously, this discovery didn't seem to be of particular interest to the scientific community at the time, or even to Walden himself, since the field of ionic liquids as we know it today truly had its start many decades later. I would argue that the fact that the first ionic liquid was protic, points to the simplicity of its synthesis, which is one of its greatest selling points. Due to this simplicity, a variety of protic ionic liquids can potentially be synthesized by combining different acids and bases (Figure 1.2). Furthermore, the structures of the cations can be modified to achieve a large variety of compounds, for instance by changing the alkyl chain length, adding functional groups, etc.[4]

3: An ionic liquid with a melting point ≤ 25°C.

4: The concept of ionic liquids being "designer solvents" [3] certainly has limits, which will be discussed further throughout this thesis.

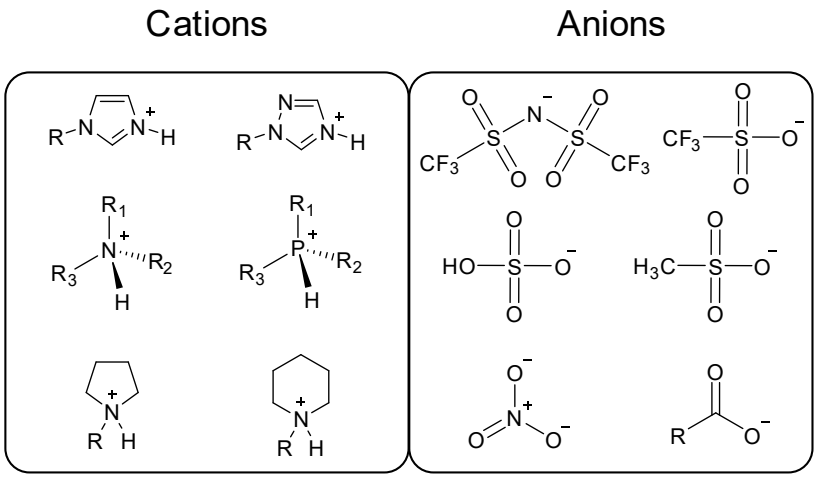

Figure 1.2: Examples of common cations and anions in protic ionic liquids.

1.2 Interests and possibilities

Although protic ionic liquids can be used in place of the more common aprotic ionic liquids for a variety of applications, most notably as solvents for many chemical processes, their most distinctive characteristic is the presence of a labile hydrogen.[5] This grants them a certain degree of Brønsted acidity, which can be exploited in different ways. Due to this acidity, protic ionic liquids have been used as dual solvent/catalyst systems for numerous chemical transformations [4]. They have also been used as lower-cost alternatives to aprotic ionic liquids in the dissolution and transformation of biomass [5, 6]. Protic ionic liquids have also been extensively researched in the context of electrochemistry, in applications such as batteries, supercapacitors [7] and, most notably, fuel cells [8, 9]. Due to the presence of an acidic hydrogen (or multiple), protic ionic liquids can hypothetically serve as proton conductors without the need for other solvents, most importantly, without the

5: This also implies that back proton transfer is possible, resulting in an equilibrium between neutral and ionic species, as will be discussed more further down.

need for water. This means that they can fulfill the role of water as a proton conductor in proton exchange membrane fuel cells (PEMFC) (Figure 1.3), allowing them to operate at intermediate temperatures, i.e. at temperatures higher than 100 °C. In practice, this could potentially eliminate the need for gas humidification systems and increase the cooling efficiency of fuel cell stacks. Operating at higher temperatures has also positive effects in regards to the tolerance of the catalyst to gas impurities as well as to faster reaction kinetics [10].

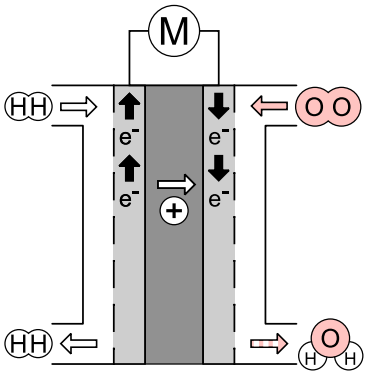

Figure 1.3: Schematic of a hydrogen-/oxygen fuel cell. This type of electrochemical device generates electricity by exploiting the two half-reactions of hydrogen oxidation and oxygen reduction at two electrodes, separated by a proton-conducting membrane.

1.3 Exploring new protic ionic liquids

Although these compounds have the potential to be used as proton conductors, a series of hurdles must be surpassed in order for that to happen. Relatively low thermal stability (higher than water, but lower when compared to aprotic ionic liquids), high viscosity and low conductivity are some of the most common problems with protic ionic liquids. Additionally, introducing these compounds to a supporting material (in order to make self-standing proton-conducting membranes for instance) can result in compatibility issues. As far as I'm aware, to date, no proton-exchange membrane systems using protic ionic liquids have been reported to surpass the power density of traditional Nafion®-based membranes [8]. This makes it clear that exploring new compounds, especially ones with higher acidity [11], could be an interesting strategy to follow.[6]

A large variety of compound structures is desirable in the field of applied chemistry, since it allows for a wider range of physicochemical properties, and in regard to the application of ionic liquids in the field of proton-exchange membranes, certain properties are extremely important. Thermal stability dictates at which temperatures the devices can operate, as well as their liquidus range.[7] The viscosity, which in turn is related to ionic conductivity will determine the efficiency of proton conduction.[8] Hydrophobicity will possibly affect the longevity of a membrane, since hydrophobic ionic liquids are less likely to leach out of the membrane due to the water produced during the operation of a fuel cell.

The development of new families of ionic liquids is evidently important for realizing the original concept of "designer solvents" [3]. In fact, the vast majority of the research being conducted in the field of ionic liquids still primarily focuses on only two families of compounds, imidazolium- and alkylammonium-based ionic liquids. I believe that this fact indicates the need for a larger variety of cation families with not only interesting physicochemical properties, but also an ease of synthesis[9] and of modifications.

6: A higher ionic liquid acidity has been shown to be related to faster oxygen reduction reaction kinetics at polycrystalline platinum electrodes [12].

7: The temperature range within which a substance is a liquid.

8: Assuming a vehicular mechanism of proton conduction. More about this in the next chapters.

9: In small and large scales, which also points to the need for keeping the chemical complexity low and using widely available precursors.

1.4 What are we trying to accomplish?

The objective of the thesis work was to synthesize new protic ionic liquids for use in proton exchange membrane fuel cells. This objective also required the development of methods for the synthesis and analysis of these compounds. Additionally, since we wish these new protic ionic liquids to be widely adopted by other research groups, we aimed at keeping the molecular complexity low, only using bases that could be synthesized with high purity (and purified using simple methods, i.e. no chromatography[10]) from commonly available precursors. This will hopefully allow many other groups to synthesize and work with these new compounds. This thesis will also explore how computational chemistry tools can be used to better understand structure-property relationships, particularly regarding acidity.

Although the fundamental objective of our work was focused on applied chemistry (having the overall intention of eventually developing new membrane materials), along the way it transformed into an exploration of the fundamental properties (and how to properly determine them) of protic ionic liquids, as it will become clear throughout the discussions in this thesis.

10: A large library of new bases could certainly be synthesized and purified by chromatographic methods; however, this would only be reasonable when working in a milligram scale, which is not interesting from the perspective of applied chemistry, where we want to be able to make several grams of compounds with high purity.

Background 2

2.1 Essential concepts in protic ionic liquids

Ionic liquids are many times generically described as having low melting points, negligible vapor pressure, low flammability, good thermochemical and electrochemical stability, and good solvation properties.[1] Protic ionic liquids can share these general characteristics to a certain extent, but as we will further discuss, the reversibility of the acid-base neutralization reaction and the presence of an acidic hydrogen in protic ionic liquids have a huge impact on their properties. Additionally, the fact that these compounds are made by this neutralization reaction, as simple as it may sound, requires some considerations.

2.1.1 Synthesis by acid-base neutralization reaction

As previously mentioned, protic ionic liquids are synthesized by an acid-base neutralization reaction. This means that in practice, in order to make pure protic ionic liquid, equal molar amounts of acid and base must be mixed. Sounds simple enough, but the challenge of measuring and fully mixing these two compounds in a controlled manner is not trivial. Acids and bases can be highly corrosive, volatile and hygroscopic (or moisture sensitive), meaning that a series of precautions must be taken to avoid introducing impurities to the resulting ionic liquid. Measuring exact molar amounts of a chemical is practically impossible, so no protic ionic liquid is truly equimolar. In reality, the acids and bases should be measured as precisely as possible in order to achieve a mole ratio of acid to base that is close to 1:1. Losses of material must also be avoided, since we must ensure that the full measured amounts of acid and base actually mixed. These difficulties usually lead to small excesses of either acid or base, which are normally the main impurities in protic ionic liquids. Another important factor to consider is that the neutralization reaction is highly exothermic, which can lead to the formation of side products, as well as to thermal decomposition. Hence, the temperature of the reaction must be kept under control. Finally, one must consider that purification procedures can also modify the composition of the protic ionic liquid by unintentionally removing either acid or base.

1: Due to these properties, they were also many times declared to be "green" solvents. These highly optimistic generic claims were mainly made during the early years of research in the field and, although true for certain ionic liquids, they are certainly not true for the entire class of compounds.

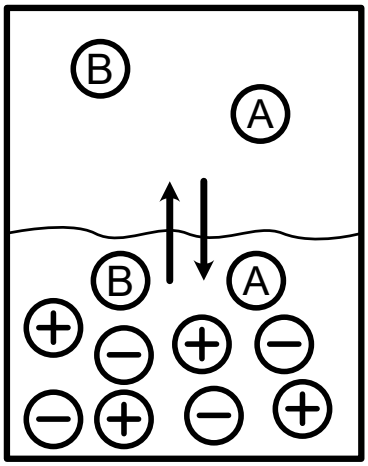

Figure 2.1: Schematic representation of the liquid-gas equilibrium in protic ionic liquids. A: free acid, B: free base, +: cation, -: anion.

As shown in Figure 1.1, the acid-base neutralization reaction that forms protic ionic liquids is reversible. The extent of this reversibility depends on the difference in pK_a (ΔpK_a) between the acid and the base. For example, mixing equimolar amounts of a weak acid and a weak base (small ΔpK_a) will result in a mixture predominantly composed of neutral species and a small number of ionic species, since the equilibrium of the acid-base reaction will be dislocated towards the reagents (commonly called pseudo-protic ionic liquids [13] or "poor" protic ionic liquids). On the other hand, mixing strong acids and bases will result in protic ionic liquids that are composed of mostly ions (commonly called true protic ionic liquids). In short, this implies that protic ionic liquids can contain both neutral (acid and base molecules) and ionic species (cations and anions) (Figure 2.1).[2] The equilibrium between these species in turn depends on temperature, with an increase of temperature leading to back proton transfer from the cations to the anions, forming more neutral species [18]. This means that increasing the temperature of a protic ionic liquid can lead to degradation, since neutral, volatile species are formed. Additionally, the volatility of these protic ionic liquids also depends on the volatility of the acid and base.

2: This aspect naturally leads to the concept of ionicity, which will not be discussed here, but has been explored at length in the literature [14–17].

2.1.2 Fundamental properties of protic ionic liquids

With an understanding of how these compounds are made, I believe that some of their fundamental properties[3] become quite intuitive. For instance, the reversibility of the acid-base neutralization reaction hints at the fact that protic ionic liquids are Brønsted acidic. If we once again focus on this reversibility, the first step in the back proton transfer reaction between the cation and the anion is the formation of a hydrogen bond, yet another fundamental concept in the field. The presence of networks of hydrogen bonds and acidic species points to the possibility of using protic ionic liquid as proton conductors. This was first demonstrated by Prof. Watanabe's group back in 2003 [19] but, after that, it has also been demonstrated that pure protic ionic liquids (with an acid:ratio of 1:1) are not capable of efficient proton conduction in H_2/O_2 fuel cells [20]. On the surface, this seems to go against the conclusions drawn by numerous other studies that successfully used protic ionic liquids as proton conductors in fuel cell systems [8, 9, 21]; however, the authors of this study [20] also demonstrate that a small excess of acid or base (which are the most common impurity in protic ionic liquids) can actually enable proton conduction. These insights support the idea of pursuing studies on non-stoichiometric protic ionic liquids [22] or mixtures of protic ionic liquids with other basic or acidic compounds [23, 24].

3: For a more extensive overview of all properties of interest in protic ionic liquids, I refer to these review articles [1, 4].

2.2 Physicochemical properties of protic ionic liquids

The fundamental physicochemical properties of protic ionic liquids are directly related to their macroscopically observed thermal and transport properties. In this thesis, I will focus the discussion on only a few properties relevant to the intended application in proton exchange membrane fuel cells.

2.2.1 Thermal properties

Understanding phase transitions and thermal stability of protic ionic liquids is essential for their potential application in fuel cell systems. In order for these compounds to operate inside devices, they must be liquids within the operating temperature range of the device (having a liquidus range between approximately -20 and 200 °C).[4] Not only that, but they must also be thermally stable, not presenting any significant decomposition at the temperatures of operation. Ionic liquids can present a series of different phase transitions, most notably the glass transition (T_g) and melting (T_m).[5] During glass transition upon cooling, the ionic liquid molecules transition from a liquid state (a supercooled, viscous liquid state) into an amorphous solid state (no structural order, with ionic liquid molecules frozen in space with no long-range order). On the other hand, during melting (upon heating), ionic liquids pass from highly ordered solids (crystalline) to a disordered liquid state.[6] Additionally, information about the intermolecular interactions within the bulk ionic liquid can be obtained from the T_g. For instance, a low T_g can indicate low attractive intermolecular interactions [28, 29]. Because of this, T_g is also intimately related to the ionic liquid's transport properties (which will be further discussed below).

The thermal stability of protic ionic liquids is usually lower when compared to aprotic ionic liquids. Another important distinction is related to the mechanism by which these compounds decompose (or vaporize[7]). In aprotic ionic liquids, many decomposition mechanisms can take place, depending on their structure [31]. In the case of these compounds, vaporization often leads to the formation of neutral ion pairs in the gas phase [32]. On the other hand, although protic ionic liquids can also degrade by the same mechanism, the first decomposition event is usually caused by the back proton transfer from the cation to the anion, forming neutral acid and base molecules that can go into the vapor phase [4, 33, 34]. Thus the thermal stability of protic ionic liquids is directly related to the

4: It is important to consider that once inside a solid supporting matrix, the thermal properties of ionic liquids can change quite significantly (confinement effects and surface interactions), with glass transition and melting temperatures being noticeably affected [25, 26].

5: Other common phase transitions include crystalization (T_c) and solid-solid ($T_{s\text{-}s}$).

6: Interestingly, certain ionic liquids can actually show some degree of nanostructuration by self-assembly even in the liquid state [27].

7: Although aprotic ionic liquids are generally considered to have negligible vapor pressures, in many cases, they can actually be distilled without decomposition [30].

ΔpK_a between the acid-base pair, as well as to the thermal stability and boiling point of the acid and the base.

2.2.2 Transport properties

The transport properties most relevant in the context of this thesis are viscosity, ionic conductivity (which includes proton conductivity) and diffusivity. Viscosity (η) is related to the resistance of the ionic liquid to flow, ionic conductivity (σ) relates to the ease with which ions are transported under the influence of an external electromagnetic field, and diffusivity (typically measured as a self-diffusion coefficient (D)) relates to the Brownian motion of the molecular species in an ionic liquid.[8]

8: These properties are related by the Nernst-Einstein (ionic conductivity and diffusivity) and Stokes-Einstein (diffusivity and viscosity) equations, as well as the Walden rule (molar conductivity and viscosity). For a general overview of these relationships, see reference [29].

Due to the protic nature of protic ionic liquids, these compounds have long been proposed to support proton conduction [19]. Two main mechanisms are commonly proposed for anhydrous proton conduction: the vehicular and the non-vehicular mechanisms.[9] As the name suggests, in the vehicular mechanism protons are conducted from one point to another like passengers in a vehicle, through the movement of protonated shuttling molecular species. In the non-vehicular mechanism, protons are conducted by being transferred from one molecular species to another, without the need for long-distance translational motion (Figure 2.2).

9: In addition, two distinct non-vehicular mechanisms are usually proposed, proton hopping and the Grotthuss mechanism. Even though many authors use these two terms interchangeably, they are two distinct mechanisms. An illustration of their differences can be found in the supporting information material of the work by Karlsson et al [35].

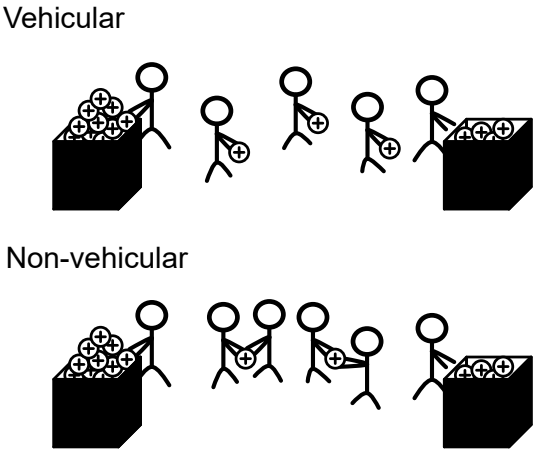

Figure 2.2: Schematic representation of the two proton conduction mechanisms discussed for protic ionic liquids.

The most common example of this type of mechanism is the Grotthuss mechanism. First proposed to explain the high proton conductivity of water, this mechanism relies on a chain of molecules connected by hydrogen bonds, where the molecular species readily donate a proton upon receiving another. This mechanism has been found in some ionic liquids [13, 36, 37] and most notably in phosphoric acid [38]. Nevertheless, the vehicular mechanism seems to be the predominant proton conduction mechanism in protic ionic liquids. Once again, it is important to point out that a recent study demonstrated that pure protic ionic liquids (specifically

protic ionic liquids with a high ΔpK_a, like [DEMA][TfO]) are not capable of supporting efficient proton conduction in H_2/O_2 fuel cells, requiring an excess of acid or base to do so [20] (or possibly protic ionic liquids with a low ΔpK_a [20, 39]).

These transport properties are derived from the interplay of different attractive and repulsive intermolecular interactions. This explains why they are dependent on temperature, since intermolecular interactions are weakened by increasing temperatures. The correlation between temperature and conductivity (or viscosity) can be described by the empirical Vogel-Fulcher-Tammann (VFT) equation:

$$\sigma = \sigma_0 \cdot e^{-(\frac{D \cdot T0}{T - T0})} \tag{2.1}$$

in which σ_0 is the ionic conductivity extrapolated for infinite temperatures, D is a parameter related to fragility (the strength parameter), T_0 is the Vogel temperature, while T is the absolute temperature expressed in Kelvin. Interestingly, by fitting conductivity data (over a range of different temperatures) with this equation, the D parameter can be extracted, which relates to the fragility of the ionic liquid.[10] This property is extremely important, since having a high fragility means that the ionic liquid's conductivity (close to T_g) is highly responsive to temperature (a small increase in temperature leads to a big increase in conductivity) [40]. A few different ways of displaying the relationship between conductivity and temperature are usually used, some of the most relevant being the Arrhenius plot and the Angell plot.

10: Fragility is a property of glass-forming materials that characterizes how rapidly the dynamics slow down upon cooling towards the glass transition temperature T_g or, vice versa, how rapidly they change upon heating from T_g [14].

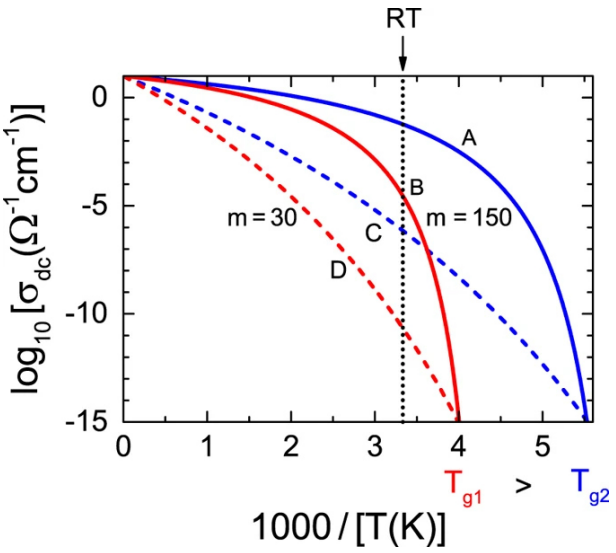

Figure 2.3: Generic Arrhenius plot of four hypothetical different glass forming compounds (A, B, C and D). The fragility of the compounds is shown by the fragility index m. Reproduced from reference [40] with the permission of the publisher under license CC.BY 4.0.

Figure 2.3 shows four hypothetical ionic glass-forming compounds with two different T_g values and two different fragility indexes (m). This image clearly shows how important it is for ionic liquids to have a combination of low T_g and high fragility, since that means that the ionic liquid will remain liquid down to very low temperatures and it will rapidly increase its conductivity as the

temperature increases from T_g. The figure also shows how two ionic liquids with the same T_g (A and C or B and D) can have drastically different conductivities at a certain temperature due to differences in fragility. Another way of interpreting fragility without the need for calculating D or m parameters[11] is by using the Angell plot (log of conductivity vs T/T_g), which is essentially a T_g-scaled Arrhenius plot.

11: $m = 16 + 590/D$[41]

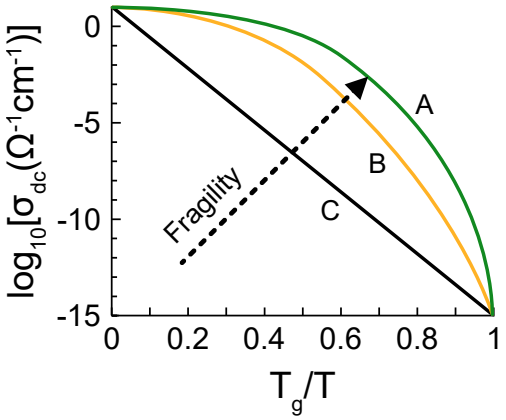

Figure 2.4: Generic Angell plot (T_g-scaled) of three hypothetical different glass forming compounds (A, B and C)..

This plot allows for the comparison of different ionic liquids as if they had the same T_g. In this type of plot, it becomes clear that generic compound A is more fragile than compound B, with C being the least fragile one (also called strong). It is also helpful to observe that the temperature increases from right to left, and as it increases, the conductivity increases at different rates for different compounds (since the curves have different slopes at $T_g/T = 1$, which is actually the definition of the fragility index m [41]).

Another important way conductivity (log of molar conductivity) can be used to determine the properties of ionic liquids (e.g. ionicity) is by plotting it against viscosity (log of η^{-1}), in a so-called Walden plot [14, 42]. Finally, diffusivity (self-diffusion coefficients) can give indications of which transport mechanism is predominant, by comparing the self-diffusion coefficients of the labile proton and non-labile protons in the cation (like ring hydrogens in the case of imidazolium-based protic ionic liquids). Diffusivity can also be used to determine ionicity [42, 43], differences in transport properties between different species in the ionic liquids, diffusion inside solid matrices, and many other properties [44].

2.3 Understanding protic ionic liquids through computational methods

2.3.1 What is molecular modeling?

As the name suggests, molecular modeling is a computational technique used to simulate molecular systems using various levels of theory (from coarse grain models to quantum mechanical models). In short, the idea is to build a geometrical representation of the system (a set of coordinates for all atoms) that accurately depicts the chemical system being studied and then calculate different properties of that system based on theoretical models. The ideal model of a molecular system would be composed of as many atoms as the real system (or as many as required to account for all long-range interactions), but that is practically impossible since it would require an absurd amount of computational power. This exemplifies the most obvious limitation of computational models: either the molecular model is big (many particles) and the level of theory is rudimentary (lots of approximations), or the molecular model is small and the level of theory is sophisticated. In practice, a lot of work is put into creating these geometrical descriptions of the molecular models, since they need to accurately represent the system being studied, but also be small enough to be computationally viable. The most popular methods for molecular modeling are based on classical (e.g. molecular mechanics, molecular dynamics) or quantum molecular mechanics (e.g. density functional theory, coupled cluster, Møller–Plesset perturbation theory). In this thesis, we will mainly explore density functional theory (DFT) based methods, since this theory strikes a nice balance between accuracy and computational cost. In regards to the molecular model, we will study isolated single ion pairs (with additional solvation models to account for some of the effects of surrounding molecules).

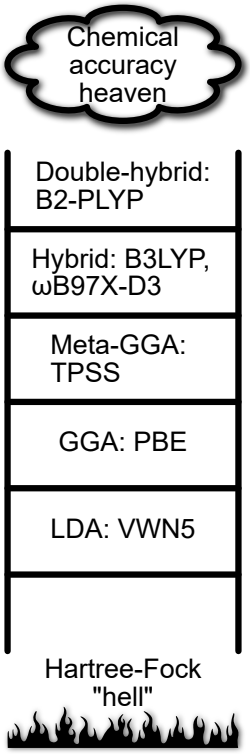

Figure 2.5: Jacobs ladder of DFT approximations (with some common functionals as examples). For more details on the differences of these methods and functionals refer to the papers by Cohen [45], Becke [46] and Bursch [47], as well as an excellent video by Prof. David Sherrill [48].

According to quantum mechanics, all the information about an atom (and by extension a molecule) is contained in its wavefunction, as described by Schrödinger's theory. Meaning that the reactivity of a molecule, its spectroscopical signatures, and many other chemical properties could be perfectly described if we knew the exact form of its wavefunction. However, this is only practical for very small systems (small number of particles), like a single hydrogen atom isolated in space. If we wish to apply these quantum chemical theories to larger systems, different approaches must be used, involving the use of some approximations. These different approaches are what I will refer to as levels of theory. Lower levels of theory make use of many approximations and are therefore further away from the "true" answer to Schrödinger's equation. On the other hand, high levels of theory can model electronic systems almost

as well as the actual Schrödinger's equation. Different models have different strategies to deal with the "many-body problem" of electronic correlation (i.e. the interaction of every electron with every other electron). Quantum mechanical models, which are generally segregated by how they deal with the "many-body problem".[12] In DFT, this gives rise to what are called functionals (which fit into different categories, depending on the level of approximation used to describe electronic correlation) (Figure 2.5). In order for these functionals to provide accurate results, they must be combined with appropriate basis sets,[13] solvation models (when required), and other corrections (like dispersion corrections). The accuracy of these methods is usually determined in reference to a "gold standard" method (usually a high level of theory method such as coupled cluster). These benchmark studies (like the excellent study from Georigk et al. [49]) serve as guides, and help in navigating the incredibly diverse variety of methods currently available.[14]

12: Systems with multiple interacting entities are notoriously complicated to compute, since every variable in the system depends on all others.

13: Basis sets are a set of primitive functions (such as Gaussian or Slater-type functions) that are combined (linear combination of atomic orbitals) to build the electronic wavefunction of a molecular system.

14: For those interested in learning more about the fundamentals of computational chemistry, I highly recommend the book "Computational Chemistry" by Prof. Jeremy Harvey [50]. Additionally, for the practical aspects of running DFT calculations, I recommend the excellent paper by Bursch et al [47].

2.3.2 Ways of modeling ionic liquids

As previously discussed, there are many different types of molecular modeling methods, from machine learning [51] to classical [52] and quantum mechanics [53]. In this thesis, we will focus on small systems; hence, we will discuss how to use DFT methods to describe their properties, and how they change in response to modifications to their chemical structure. In an ideal model of a protic ionic liquid, multiple ion-pairs (and additionally neutral species, i.e. acid and base) would be used to build the model, maybe hundreds or thousands of molecules, perfectly representing the solvation and long-range intermolecular effects. However, as previously discussed, this is not possible with high level DFT methods. Most commonly, single ion pairs are used, and to account for some of the solvation effects, implicit solvation models are used.[15] Ionic liquids are usually very flexible molecules, transitioning between many low-energy conformers. Ideally, ensemble methods would be used, selecting a wide range of conformers, in order to better represent the bulk state of the ionic liquid. If that is not possible, choosing the lowest energy conformation of the ionic liquid is the next best option (since this low energy conformer will have the highest probability of being present in the bulk, according to the Boltzmann distribution). This can be quite difficult, since ionic liquids have a very "smooth" conformation space (many low-energy conformers). To better understand this problem, let us look at the example of the two hypothetical dimer systems (Figure 2.6). First, consider dimer A. The puzzle pieces can easily fit in multiple different ways, therefore, their relative energies will be

15: In this model, the Coulombic effects of the solvent on the studied molecules are approximated by surrounding the molecule with point charges.

quite similar and the barriers to transition between the different dimer configurations (conformers) will be very low ("smooth" potential energy surface). On the other hand, if we look at the key and lock (dimer B), there is only one obvious way they can fit, making the other higher energy configurations less favorable and harder to access ("rough" potential energy surface).

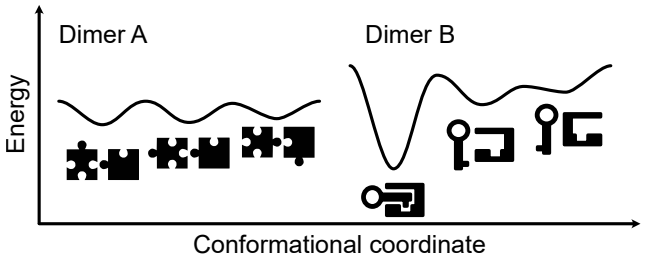

Figure 2.6: Scheme of two different one-dimensional potential energy surfaces for two different dimer systems.

2.3.3 Molecular descriptors and computational analysis

With an optimized ion-pair geometry in hand, the next step is to calculate the properties of interest. The IR vibrational spectrum (Raman can also be additionally calculated) is one of the properties immediately available, since a vibrational analysis (using the rigid-rotor-harmonic-oscillator approximation [54]) is required to achieve a truly optimized structure. Also, since we now have an optimized geometry, geometrical information such as bond lengths are also available. Partial atomic charges (using the CHELPG scheme for instance [55]) and electronic potential maps can also be calculated and used to determine charge distribution along the molecule. The energetics of the molecule are also easily extracted from the computational chemistry software's output file (although the use of some of these energies may require certain corrections due to the basis set superposition error [56]). Some of the most useful pieces of information about these systems are the frontier orbital energies (HOMO and LUMO). Within the framework of conceptual DFT (CDFT), HOMO and LUMO energies can be used to determine electronegativity (χ), hardness (η), and electrophilicity (ω) [57, 58] using these equations:

$$\chi = -\frac{\epsilon_{\text{HOMO}} + \epsilon_{\text{LUMO}}}{2} \tag{2.2}$$

$$\eta = \epsilon_{\text{LUMO}} - \epsilon_{\text{HOMO}} \tag{2.3}$$

$$\omega = \frac{\chi^2}{2\eta} \tag{2.4}$$

These molecular descriptors can be used to determine differences in the Lewis acidic (which is correlated with Brønsted acidity as well [59]) character of different molecules. The wavefunction

output file can also be used in conjunction with other software (most notably MultiWFN [60]) to determine hydrogen bonding energies [61],[16] within the framework of the atoms in molecules theory (AIM) [63].

16: Although the popular Espinosa method for estimation of hydrogen bonding strength was used in this thesis, recently better methods have been proposed [62].

Finally, it is important to discuss some considerations about the use of computational molecular modeling techniques. When interpreting the results, one must consider that all models have limitations. In the case of this work, as discussed previously, the molecular models used (isolated ion-pairs with implicit solvation) are not an absolutely true representation of the bulk phase of protic ionic liquids, but an approximation. Also, the quantum chemical models themselves are not perfect, not achieving the "chemical accuracy heaven" (Figure 2.5). Although these methods are not usually capable of perfectly predicting experimentally determined observables (such as bond lengths and vibrational frequencies for example), they can certainly get extremely close, making them useful tools for determining general trends between a series of compounds. In short, computational results should always be taken with a grain of salt, and are better interpreted in conjunction with experimental data.

Methodology 3

3.1 What to consider when making and analyzing protic ionic liquids?

To start answering this question, we must first consider that in some ways, making protic ionic liquids is no different from making any other new organic compound. We must first synthesize the intended compound, making sure that it has the intended chemical structure. If we now want to determine its properties, we must do so without modifying it in the process; otherwise, we are not truly analyzing its intrinsic fundamental properties.

So, in which ways are protic ionic liquids different from regular organic compounds? As previously discussed, they are made by mixing equimolar amounts of acids and bases. Once again, to truly achieve an equimolar mixture of two compounds is impractical, so we should strive to achieve a ratio that is as close as possible to 1. Accurately measuring these compounds without modifying them is also not trivial; they can be corrosive, volatile, and hygroscopic. Impurities must also be considered, since no compound is 100% pure. Okay, let us assume that we now have two different containers with accurately measured, unadulterated acid and base, which we must now completely mix. This means, that every single drop of both compounds must be accounted for, with only negligible losses. This mixing must also be done slowly and at low temperatures, to avoid any undesired side reactions or overheating.[1] Finally, we must consider whether purification procedures should be conducted or not. There are quite a few limitations on what types of purification procedures can actually be performed in protic ionic liquids, since they cannot usually be purified by simple traditional methods, like distillation, solvent extraction, and recrystallization. Two very common purification methods involve the use of molecular sieves to remove water and activated charcoal to remove colored impurities. Both must be carefully considered and conducted, since they can lead to the introduction of new impurities [64]. In traditional organic synthesis, many of these problems can be solved by the use of a solvent, but this introduces other issues in the synthesis of protic ionic liquids. Overall, it's important to understand that ionic liquids require special consideration in regard to synthesis and purification.[2]

Assuming that we have a pure protic ionic liquid that is stable and stored under appropriate conditions, how do we analyze it

1: I speculate that even the order of addition (acid to base or base to acid) can have an effect on the final product.

2: For the purification and synthesis of aprotic ionic liquids, see references [65, 66].

without changing it in the process? The answer will of course depend on the type of analysis, but the basic principle that must be followed is that the compound must be unaltered during the analysis (unless the analysis is destructive of course, in which case the sample should be unaltered until the moment where it will be analyzed). Therefore, some of the same concerns that arise when making protic ionic liquids will be relevant also during the process of characterization (corrosion, thermal decomposition, water absorption, etc.).

3.2 Avoiding moisture contamination with air-free techniques

The use of inert atmospheres and air-free techniques is essential to make and analyze these compounds, since one of the most apparent properties of ionic liquids is their ability to absorb water from their surroundings (hygroscopicity). The effects of water in ionic liquids have been studied in length since the early days of the field [67] and it can exert drastic impacts on most properties, like viscosity, conductivity, etc. To avoid the interference of water, air-free Schlenk techniques [68, 69] and glovebox systems can be used. While Schlenk systems are significantly more accessible for most researchers, the higher cost of glovebox systems can be justified since they allow for the manipulation of these compounds under a highly controlled atmosphere. There are many benefits of working under such a controlled environment (reproducibility of results, long-term storage stability, etc.); however, this environment also introduces a series of constraints to experimental setups (space, temperature control, limited mobility, etc.). The details on how each synthesis and analysis technique was adapted to avoid moisture contamination are further discussed in the next sections, as well as in Papers I, II and III.

3.3 Our approach for making protic ionic liquids

Every time we contemplated the idea of making a new ionic liquid, a few considerations were taken. Due to the application we had in mind (proton conductors in proton exchange membrane fuel cells), the ionic liquids should have high purity (as high as we could achieve reasonably), should be liquid, its synthesis should be reproducible, scalable (anywhere in the range of 1 to 20 g should be easily within reach) and if possible, solvent-free.[3] Regarding the choice of acid, we decided to focus on using trifluoromethanesulfonic acid (HTfO, also known as triflic acid)

3: The solvent-free synthesis of protic ionic liquids is only possible if at least one of the components is a liquid; otherwise, an easily removable solvent should be used.

and bis(trifluoromethane)sulfonimide (HTFSI), since both of these strong acids are commercially available in high purity, and can form thermally and electrochemically stable protic ionic liquids. Protic ionic liquids based on the bis(trifluoromethane)sulfonimide anion (TFSI) usually have higher ionic conductivity when compared to other anions (due to its low intermolecular interactions with the cations and its flexibility [70], reducing viscosity), as well as potentially being hydrophobic, which is interesting for their application in fuel cells.

3.3.1 Considerations when designing and synthesizing a new base

Due to the previously discussed considerations, the synthesis of the bases must also follow certain criteria. We wanted to make sure that other research groups could replicate our work, so we focused on keeping the complexity of the bases low, meaning that they must be synthesized from simple, commercially available precursors in only a few synthetic steps. They must be able to be produced in decent amounts (at least 10 g at a time),[4] with high purity and without the need for complex purification procedures (no chromatographic methods, ideally purified by distillation or recrystallization). Finally, it's important that these bases contain only small amounts of moisture (preferably under 1000 ppm), since this moisture will get carried to the resulting ionic liquid, where it can be harder to remove. This can be easily determined by Karl Fischer titration before the bases are permanently stored inside the glovebox. In general, the synthesis of all bases was done by a simple alkylation reaction using alkyl halides (Figure 3.1). Although simple, the reaction conditions and purification procedures for each one of the bases had to be carefully considered to increase the yields and produce only the desired products. More details on this can be found in Papers I and III, as well as in later sections of this thesis.

4: While a larger variety of bases could be synthesized in the milligram scale (and purified by chromatographic methods), scaling up is usually impractical. However, this could be a valid strategy for making a large variety of compounds from a matrix of acids and bases. Work on the use of automated high throughput systems to perform these types of synthesis has been recently reported [71].

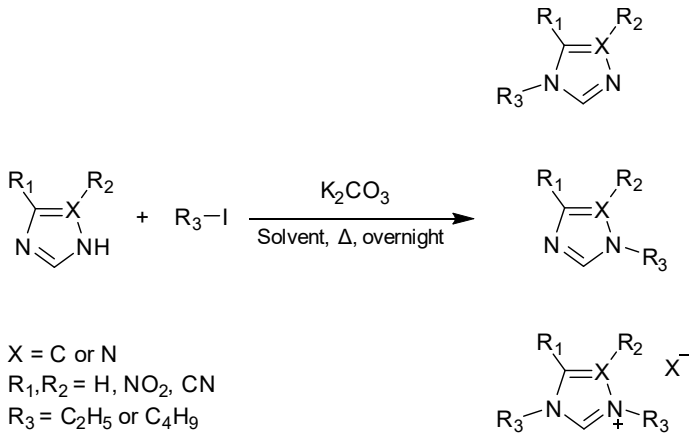

Figure 3.1: Generic synthesis scheme for all bases synthesized in this thesis.

3.3.2 The concept of the synthesis setup

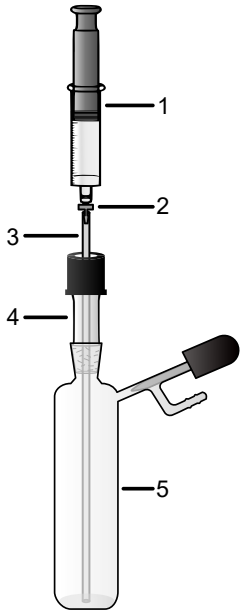

Figure 3.2: The setup developed for the synthesis of protic ionic liquids. (1) 10 mL gas-tight glass syringe with PTFE plunger seal, (2) PVDF adapter, (3) PTFE tube, (4) thermometer adapter, and (5) 25 mL Schlenk vial.

5: Accuracy is more difficult to achieve, especially for solids.

Paper I describes how a synthesis setup was constructed to take into account all of the constraints previously discussed (as well as some others, further discussed in Paper I). In short, the setup (Figure 3.2) consists of two main modules, the syringe module (parts 1, 2, and 3) and the Schlenk module (parts 4, 5, and a stir bar). Liquids can be accurately and precisely measured (by weight) on the syringe module, while solids or liquids can also be precisely[5] measured (by weight) on the Schlenk module. This setup is assembled and filled with reagents inside a glovebox, which is necessary to avoid atmospheric moisture. Once both modules are filled with the appropriate amounts of reagents, they can be connected (through parts 3 and 4). The system is then removed from the glovebox and connected to a nitrogen Schlenk line. At this point, the Schlenk vial is cooled down with an ice bath (which is the reason why at the time we worked on the research from Paper I, the reaction was not conducted inside the glovebox. This changed for the work in Paper III, as will be discussed in the next section) and placed on top of a heating plate with magnetic stirring. Cooling is necessary to avoid heat decomposition and side reactions, since the neutralization reaction is very exothermic. The reagents can now be slowly mixed by pressing down on the syringe plunger. To make sure that no unreacted compounds are left on the walls of the system (or inside the PTFE tube for example), the liquid on the Schlenk vial is pulled back to the syringe and recirculated through the whole system multiple times, guaranteeing that both components (acid and base) are fully mixed. Now the protic ionic liquid is ready to be brought back to the glovebox, where a final purification procedure is performed before storage (using activated charcoal and molecular sieves). This procedure resulted in pure protic ionic liquids with very low water contents (Table 3.1). More details on this procedure can be found in Paper I, as well as in a video in its supporting information.

Table 3.1: Purity assay and water content of the protic ionic liquids from Paper I.

Protic ionic liquid	Purity assay (% m/m from ^{19}F-qNMR)	Water content (ppm)
$[C_2HTr_{1,2,4}][TfO]$	98.0	345
$[C_2HTr_{1,2,4}][TFSI]$	98.3	553
$[C_2HIm][TfO]^a$	99.7	bdl^b
$[C_2HIm][TFSI]$	99.1	128

[a]From IoLiTec; [b]bdl: below detection limit

3.3.3 Upgrading the synthesis setup

This synthesis setup described in Paper I is by no means perfect, having a series of limitations. Our intention with Paper I was to bring the issue of synthesizing protic ionic liquids to the spotlight, in the hope that the community would improve our setup (or even create a different, better one) while considering the requirements and constraints previously discussed. One of the obvious limitations of our setup was the need to remove it from the glovebox in order to cool it. This cooling step cannot be easily achieved inside the glovebox without creating highly customized systems. One solution to this problem is to use a magnetic stirrer plate with heating and cooling capabilities, which is the case of the Polar Bear Plus system by Cambridge Reactor Design Ltd [72]. This equipment can easily be placed inside the glovebox, without any modifications required (either to the equipment or to the glovebox) and can operate between the temperatures of -40 to 150 °C (as long as the temperature of the glovebox doesn't exceed 34 °C). With the aid of this system, the ionic liquid synthesis setup doesn't have to leave the glovebox at any step, which avoids the risk of exposing the ionic liquid to atmospheric moisture and drastically simplifies the synthesis. This equipment was also used to perform the conductivity measurements described in Papers II and III. Another significant change in our synthetic procedure between Papers I and III is the introduction of a solvent in one of the syntheses. In fact, a big limitation of our setup is that it requires at least one of the precursors to be liquid; hence, if two solids need to be mixed, a solvent is required. We chose dichloromethane, since it dissolved our base quite well, it is unreactive towards both precursors and can be removed at low temperatures due to its low boiling point. This is obviously not ideal, since it can leave solvent residues in the ionic liquid (although we were not able to detect any in the ^{1}H- and ^{13}C-NMR spectra of the resulting ionic liquid).

3.4 Characterization and property analysis

Before discussing the analytical techniques used in this thesis work, it's important to once again point out that they were all designed to be air-free, in order to avoid as much as possible contact with atmospheric moisture. Our objective was to ideally analyze the ionic liquids in the same state as they are inside the glovebox, pure and unmodified.[6]

A series of analytical techniques were used to determine a variety of properties, but in general, we are trying to answer a few questions. Is the structure of the ionic liquid what we expect it

6: Gas chromatography (for the determination of base purity) and Karl Fischer titration (water content) were used in the thesis work and are not going to be mentioned in detail here. They are less relevant to the work and they were not significantly adapted. Experimental details about these techniques can be found in Paper I.

to be? Is it reasonably pure? What are the phase transitions and thermal stability? How do differences in the structure affect acidity, intermolecular interactions, conductivity, and self-diffusion?

3.4.1 Spectroscopic analysis

Spectroscopic analysis relies on the interaction of matter with electromagnetic radiation. In this thesis work, three types of spectroscopic methods were used: nuclear magnetic resonance spectroscopy (NMR), Fourier-transform infrared spectroscopy (FTIR) and Raman Spectroscopy.[7]

7: It's not my intention to give detailed explanations on how these well-known analytical techniques work, since there are excellent resources elsewhere. A basic understanding of these techniques is expected from the reader, hence I will focus on explaining how these techniques were adapted to analyze the protic ionic liquids at focus in this thesis.

Nuclear magnetic resonance spectroscopy

NMR spectroscopy exploits a quantum property called nuclear spin (in the case of this work we were only interested in the ^{1}H,^{13}C and ^{19}F nuclei) to gather molecular chemical information from both cation and anion. Under the influence of a strong magnetic field, these nuclei respond to electromagnetic pulses in different ways, depending on their electronic environment (depending on what other atoms are around them); hence, this can be used to extract all sorts of chemical information. It can be used to determine molecular chemical structure, quantify species, compare Brønsted acidity, or determine how different species diffuse (more about this in another section below).

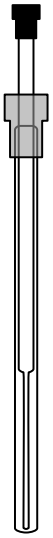

Figure 3.3: Coaxial NMR tube. The outer tube contains the pure protic ionic liquid, while the inside capillary contains DMSO-d_6 with TMS.

In regard to the practical aspects of preparing ionic liquid samples for NMR analysis, it is necessary to point out that water has an influence on the chemical shifts of protic ionic liquids, especially on the shift of the NH hydrogen [43]. In order to avoid that, samples were always prepared inside the glovebox, sealed, and analyzed as quickly as possible. The chemical shifts of the ionic liquid are also dependent on the influence of the solvent, hence, samples were analyzed as pure liquids with the aid of coaxial NMR tubes (Figure 3.3) filled with DMSO-d_6 with TMS (in the inner tube) for locking and referencing. Additionally, some ionic liquids (from Paper III, specifically) had to be heated to 60 °C during the acquisition of the NMR spectra, in order to reduce their viscosity and significantly improve the spectral resolution.

NMR spectroscopy can be used not only qualitatively, in order to confirm the structure of the protic ionic liquids (and also to determine the absence of some contaminants), but also quantitatively. Importantly, to perform this type of quantitative analysis, the NMR spectra must have been acquired under quantitative conditions. In quantitative NMR (qNMR[8]), the signals are collected in a way that ensures that their peak areas are related to the concentration of the

8: A good review on all aspects of qNMR was written by Bharti and Roy [73]; hence, in this thesis, there will only be a short discussion on the most crucial aspects to consider when performing this type of analysis.

species producing that signal. This means that this technique can also be used to conduct purity essays by using an internal standard (a molecule that will serve as a reference of signal area per unit of nuclei) of known quantity and purity. Many things need to be considered when performing this type of analysis, but the first step is to choose an appropriate internal standard. It must have a simple NMR spectrum and have at least one peak (preferentially a singlet, since its integration is simple and accurate) that does not overlap with the analyte's peak of interest. This standard should be soluble in the NMR solvent of choice, non-reactive, non-hygroscopic, non-volatile, easy to handle (since the compound has to be precisely weighted, liquids with low volatility are quite well suited for this application), and of high purity. For the quantitative data presented in Table 3.1 (Paper I), 4-fluoroacetophenone was used. Triplicate samples (of protic ionic liquid mixed with 4-fluoroacetophenone in DMSO-d_6) were prepared and sealed inside the glovebox in order to reduce experimental errors and avoid moisture. These samples were analyzed by ^{19}F-qNMR, since it yields spectra with very well-resolved and strong singlets. These spectra were acquired and analyzed under suitable conditions (in order to get quantitative conditions, see details in Paper I), which were in turn used to calculate purities by the following equation:

$$P_x = (A_x/A_s)(N_x/N_s)(W_x/W_s)(M_x/M_s)P_s \tag{3.1}$$

where A_x and A_s are the peak areas of the analyte (x) and standard (s), N_x and N_s are the number of fluorine atoms of the analyte and standard molecules, W_x and W_s are the mass amounts of analyte and standard, M_x and M_s are the molecular masses of analyte and standard, and finally P_x and P_s are the purities of analyte and standard.[9]

9: This is conveniently implemented as a script in the MestReNova software [74].

Fourier transform infrared spectroscopy

Molecules can interact with infrared (IR) radiation by absorbing it and converting that energy to molecular vibrations (heat). Since these vibrational modes are quantized, only specific wavelengths can be absorbed. This absorption behavior depends on the molecular structure of the compound being excited, therefore, this type of spectroscopy provides a unique fingerprint for every molecule, and can provide a variety of other meaningful chemical information [75]. In FTIR spectroscopy, the sample is irradiated with polychromatic IR radiation from an interferometer, which is then transmitted through the sample and collected by a detector, forming what is called an interferogram. Using a mathematical operator called the Fourier transform, this interferometer can be used to build a spectrogram. Many different sampling techniques

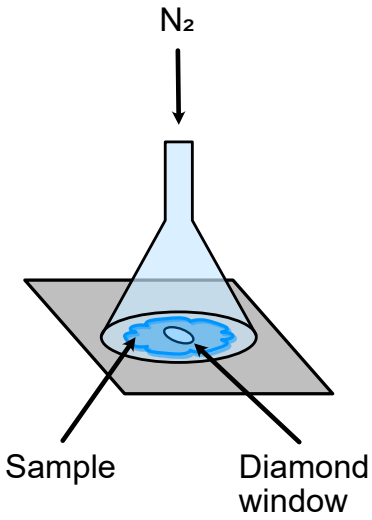

Figure 3.4: FTIR-ATR funnel setup.

can be used to expose the sample to IR radiation, but one of the most common and simple ones is called ATR (Attenuated Total Reflection). In this type of instrument, the sample is placed on top of a crystal (usually a diamond) which is irradiated with IR. Most of this radiation is simply reflected inside the crystal, but part of it is absorbed by the sample material on top of the crystal. In order to perform this type of analysis without the influence of atmospheric moisture, samples of the ionic liquids were collected from the glovebox in sealed syringes and placed on the ATR's diamond window under flow of dry nitrogen gas using a funnel (Figure 3.4).

Raman spectroscopy

Raman spectroscopy operates by a different excitation mechanism, and results in spectra with different characteristics, although the fundamental molecular vibrational modes detected are the same.[10] Different from FTIR methods, in Raman spectroscopy, a phenomenon called Raman scattering is exploited to generate a signal. In order to create this Raman signal, the sample must be exposed to radiation with higher energy than the one associated with the molecular vibrational modes (since these vibrational states are produced by interacting with IR radiation, the Raman excitation source must be of higher energy). A series of different lasers with wavelengths from ultraviolet to visible are commonly used for this purpose. The choice of laser is quite important, since some samples can exhibit fluorescence at certain wavelengths, which can drown the weak Raman scattering signals. A few different things can happen when these molecules interact with these high energy (compared to IR radiation) photons (Figure 3.5). A ground state molecule can be excited to a higher energy level (called a virtual energy state) and simply decay back into that same state producing Rayleight scattering. If instead of decaying to the ground state this molecule decays to a level above the ground state by emitting a red-shifted photon, it will produce Stokes Raman scattering. The other possibility is that the incoming radiation hits a molecule that is already excited, which means that when decaying back to the ground state, the molecule will emit radiation that is blue-shifted, producing the Anti-Stokes Raman scattering. This red-shifted radiation (Stokes) is usually detected (since at room temperature it is more intense compared to the Anti-stokes radiation) and used to form a spectrogram. Importantly, the Raman measurements were conducted using a Raman microscope (which is simply a Raman spectrometer connected to an optical microscope), meaning that samples have to be contained under the objective lenses (at the focal plane) of an optical microscope. In the same way that water can interact with the analytes and affect their FTIR spectra, it can affect

10: While the vibrations are the same, depending on molecular symmetry, some are only visible on Raman for instance, being called Raman active. The same can happen on FTIR, being called IR active.

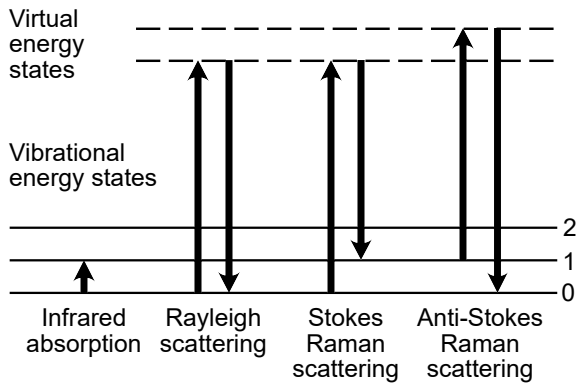

Figure 3.5: Jablonski diagram for different absorption and scattering modes on vibrational spectroscopy. Based on the work by Wikipedia user Moxfyre [76].

the Raman spectra as well. Therefore, all samples were prepared inside the glovebox and placed inside a specially designed (by Dr. Mohammad Hasani) sample holder (Figure 3.6). Samples can also be analyzed inside common NMR tubes, but it can result in issues related to the Raman signals from the glass walls of the NMR tube.

3.4.2 Thermal analysis

In the context of this thesis work, thermal analysis was used to determine the thermal stability of the protic ionic liquids, their liquidus range, and to aid in the understanding of their transport properties (by the use of T_g in conjunction with conductivity data). Due to the intended application of these ionic liquids, they must be stable and liquid in a wide range of temperatures. To determine their thermal stability, thermogravimetric analysis (TGA) was conducted, while to analyze their phase transition behavior, differential scanning calorimetry (DSC) was used. Indeed, this will sound a bit repetitive, but once again, atmospheric moisture must be taken into consideration when preparing and analyzing samples of these compounds.

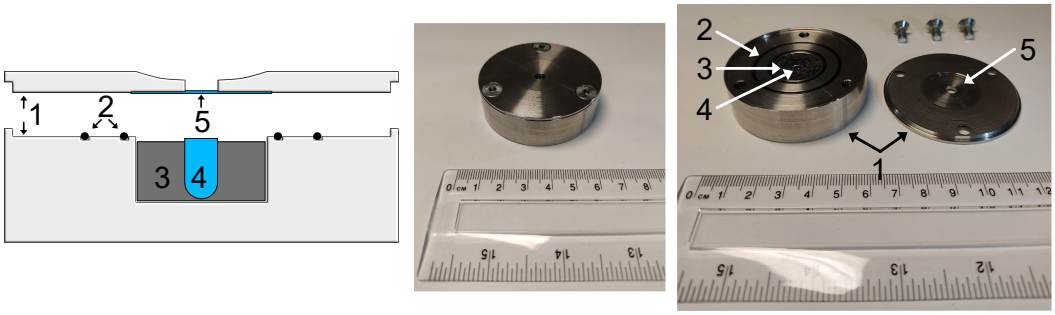

Figure 3.6: Custom-made air-tight cell. (1) Stainless steel body and lid, (2) rubber o-rings, (3) foam tube support, (4) glass tube (bottom part of an NMR tube), (5) round glass coverslip (fixed to the lid with silicon grease).

Thermogravimetric analysis

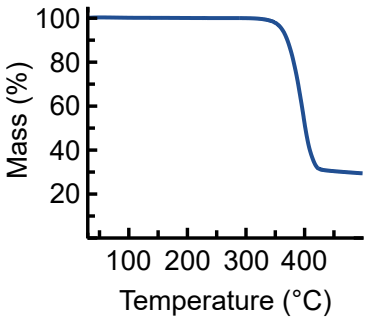

Figure 3.7: Example of a TGA thermogram; in this case, the thermogram for $[C_2HIm][TfO]$.

In TGA, a small sample of analyte (placed inside a small open crucible, usually made of aluminium) is heated at a controlled rate on top of a precision scale, which will record the weight change over time. As the sample increases in temperature, vaporization of volatile compounds and thermal decomposition (leading to the formation of gaseous by-products) will lead to a decrease in the sample mass (although some samples can increase due to oxidation, depending on the atmosphere surrounding the sample). This change in mass can be plotted as a function of time, forming a TGA thermogram (as an example, see Figure 3.7).

Crucially, in Paper I, we discussed how the way the samples are analyzed can have a significant effect on the results. One common practice in the ionic liquid literature is to perform a drying step (inside the TGA instrument) on the sample before it is analyzed, in order to remove absorbed moisture. This can be considered appropriate for some thermally stable aprotic ionic liquids, but protic ionic liquids can suffer significant thermal decomposition at temperatures around 100 °C (120 °C for 30 minutes is a common way of drying samples before analysis). If such a treatment is conducted, it is extremely important to report it, since it will modify the results. Another consideration is the atmosphere inside the oven. Samples can be reactive towards oxygen at elevated temperatures, hence, most TGA analyses happen under N_2 atmosphere, which is generally inert. This is however not how a sample would behave under normal conditions (under regular atmosphere). It is also important to consider that regular TGA experiments happen in a few hours at most (with moderate heating rates), meaning that they are not representative of the long-term thermal stability of compounds. For instance, if we look at Figure 3.7 we will notice that no significant change in the sample mass can be detected up to around 350 °C; however, if the same sample was analyzed by isothermal TGA (TGA at constant temperature) at 250 °C, a certain amount of mass loss should be expected over a long experimental period.[11] Even the choice of material of the crucible can affect the results [79]. Finally, when reporting TGA results, it is important to not only provide the onset decomposition temperature, but to provide the full thermograph as well as the peak decomposition from the first derivative of the TGA curve.

For our experiments, no pre-heating treatment was conducted (only conducted in Paper I, to show the effect of this heating treatment), and to avoid absorption of moisture, the samples were prepared inside the glovebox and introduced into the instrument under nitrogen flow from a hose (by following the sample with a hose until the moment it was inside the instrument). The specific

11: This loss of mass has been demonstrated for aprotic ionic liquids [77], and should be considerably more pronounced for protic ionic liquids [78], due to the reversibility of the acid-base reaction that forms them.

details of how each sample was analyzed can be found in Papers I and III.

Differential scanning calorimetry

In DSC analysis, a sample of analyte is submitted to heating and cooling cycles while the heat flow to the sample is recorded. This technique is commonly used to detect phase transitions, since they usually result in the release or absorption of heat (exothermal and endothermal). Transitions can also result in a change in the heat capacity of the sample. The heat flow can be plotted as a function of the sample temperature, creating a DSC thermogram (Figure 3.8).

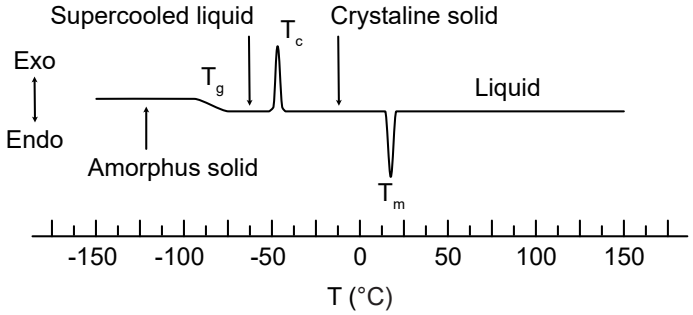

Figure 3.8: Example of a generic DSC thermogram for an ionic liquid being heated at a constant rate.

This figure is an oversimplification of the shape of a true DSC curve since, in reality, artifacts and other events can trigger changes in the heat flow, making a real DSC curve a bit more complex. This illustration shows how some of the main transitions for ionic liquids can be identified, with T_g being observed as a change in heat capacity, T_c as an exothermal peak, and T_m as an endothermal peak.[12] Importantly, DSC is notoriously sensitive to experimental variables (heating/cooling rates, crucible material, sample physical state, sample size, sample history, etc.), hence, it is important to analyze samples under the same conditions. Some properties like T_g are particularly sensitive, changing drastically with heating/cooling rates for instance. To deal with some of these issues, samples are usually submitted to at least two heating and cooling cycles, and the data reported usually doesn't come from the first cycle. Additionally, the appearance of certain transitions depends on the heating/cooling rates. For instance, samples that are rapidly cooled from the liquid state, are more likely to supercool and form glasses. On the other hand, samples that are slowly cooled, can have enough time to form crystalline structures.

12: Other transitions that are not relevant to this thesis can happen as well, such as solid-solid transitions.

In this thesis work, samples were analyzed in sealed (prepared inside the glovebox) aluminium crucibles, which avoids the issue of moisture absorption. In Paper I, two different methods (with fast and slow cooling rates) were compared, while in Paper III only one heating/cooling rate was used, in order to favor the detection of the

glass transition. Further details about the experimental procedures can be found in Papers I and III.

3.4.3 Transport properties

Pulsed-field gradient NMR spectroscopy

While the theory behind Pulse-field gradient NMR (PFG-NMR) is too complicated to properly explain here,[13] the idea is to create a position-dependent NMR signal inside the NMR sample. This is accomplished by using a pulsed gradient field (a short pulse electromagnetic field that has varying strength along the axis of the NMR tube). This can be used to produce a signal that will decay (by different amounts depending on the strength of the field) only if the interacting nuclei are moving/diffusing (by Brownian motion), due to the dephasing of the nuclei's transverse magnetization vectors. The intensity of this decay (expressed by the intensity of the signals with and without the influence of the pulsed gradient field) can be used to calculate self-diffusion coefficients (D) by using the Stejskal-Tanner equation [82]:

13: These references are excellent resources to learn more about the fundamental theory behind PFG-NMR and NMR in general [80, 81].

$$I = I_0 \times e^{-D(\gamma g \delta)^2(\Delta - \delta/3)} \tag{3.2}$$

where I is the signal intensity, I_0 the signal intensity at zero gradient, Δ the diffusion time, δ is the gradient pulse duration, γ is the gyromagnetic ratio of the nucleus studied, and g is the gradient strength. By plotting the intensity of this decay ($\ln(I/I_0)$) vs k ($k = (\gamma g \delta)^2(\Delta - \delta/3)$), the slope of the resulting curve will be the D of the species associated with that signal.

This analysis can be performed for multiple different nuclei, which allows for the quantification of the D of different species. In the case of the work presented in Paper II, self-diffusion coefficients were estimated for four distinct nuclei; i.e. the alkyl chain hydrogens, ring hydrogens, NH hydrogen, and anion fluorine. This was done in order to observe possible differences in the self-diffusion of different species within the same ionic liquid (which will be further discussed in the results and discussion section of this thesis).

The samples for this analysis were exactly the same as the ones used for regular qualitative NMR (Figure 3.3). Details about the parameters used can be found in Paper II.

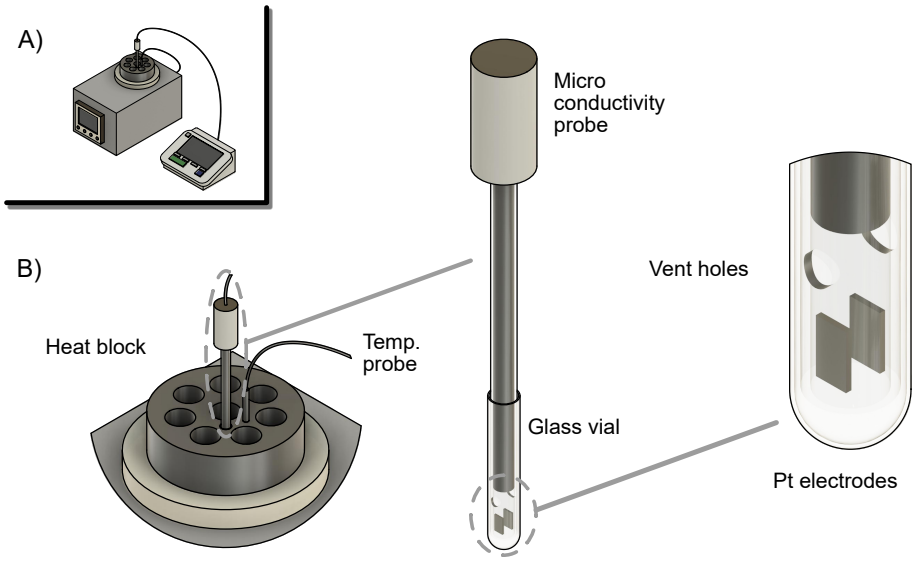

Figure 3.9: Ionic conductivity setup. (A) The entire setup inside the glovebox. Polar Bear Plus to the left, conductivity meter to the right. (B) Zoomed-in details of the components of the setup.

3.4.4 Ionic conductivity measurements

The ionic conductivity of protic ionic liquids is very sensitive to variations in moisture content, therefore, all measurements reported in this thesis (Paper II and III) were performed using a custom conductivity setup placed inside a glovebox (Figure 3.9). Our objective was to create a setup that would allow us to perform conductivity measurements in small volumes of ionic liquid (<0.5 mL)[14] at a range of different temperature and without the influence of atmospheric moisture. In order to achieve temperature control, the Polar Bear Plus device was used, operating at temperatures between 25 and 80 °C (temperature range chosen due to the limitation set by the probe, which is rated to operate between 0 and 100 °C). Ionic liquid samples were placed inside small glass test tubes, which were inserted inside a heat block with a thermocouple placed next to the sample. A microconductivity probe was used (parallel platinum electrodes) in conjunction with a benchtop conductivity meter[15] (which was calibrated outside the glovebox using an aqueous conductivity standard in the range of conductivity of the ionic liquid samples). The variation in the measured values was estimated using triplicate samples of the aqueous conductivity standard and a commercial protic ionic liquid ([C_2HIm][TFSI] from IoLiTec), resulting in a standard deviation of 0.02 and 0.002 mS/cm respectively. More details on this setup can be found in Paper II.

14: Since we wanted to analyze small volumes of leftover samples from the work in Paper I.

15: An important limitation of this setup is that the instrument does not provide any information (or control) on the frequency of AC voltage applied to the sample, and ionic conductivity is dependent on this frequency. Still, the values measured were quite reasonable and comparable with the literature. Ideally, this setup would be benchmarked against results from other techniques, like broadband dielectric spectroscopy (BDS), which measures conductivity over a range of frequencies.

3.5 Molecular modeling

There are three fundamental steps in the molecular modeling work conducted in this thesis work: the choice of level of theory, the elaboration of a molecular model, and the final analysis of the computational data. Since the field of computational chemistry is constantly evolving (with the development of new functionals, semi-empirical methods, geometry search algorithms, etc.), the methods used in this thesis work changed from Paper I to Paper III. Additionally, these changes also reflect my own personal development in the field. In the next sections, I will try to explain how these methods were selected and used to answer fundamental questions about the chemical properties of the ionic liquids discussed in this thesis.

3.5.1 Choosing a level of theory

The level of theory used will determine the accuracy of the energetic calculations conducted, as well as their computational cost. Therefore, a mix of low- and high-level methods was used to achieve a good balance between accuracy and computational cost. As previously discussed, I chose to model these ionic liquids as simple ion pairs, a popular approach that certainly has its limitations[16], but is quite effective at providing insight into how modifications in the structure of these ionic liquids change their electronic structures.

16: The limitations of such an approach have been discussed in reference [53]. Ionic liquids can certainly be modeled as larger clusters of hundreds of molecules using low levels of theory [52], but attempting to perform high-level of theory calculations even with modest clusters (a few ion pairs) is not a trivial task [83]. Interestingly, new multi-layer (using multiple levels of theory in the same calculation of a cluster of molecules) approaches are available nowadays [84], but are yet to become popular in the field of ionic liquids [85].

There is an incredible diversity of levels of theory available nowadays. Hundreds of semi-empirical methods, DFT functionals and basis sets. On top of that, several approximations and corrections can be added to the calculations. Choosing between all of these methods can feel overwhelming, but there are excellent resources to help navigate this field [47, 50]. Benchmark studies are some of the most valuable studies in the field of computational chemistry [86], since they allow for the direct comparison of the accuracy of various methods. In short, these types of studies compare the results of a series of calculations (different properties calculated for different compounds using different functionals) to the results obtained from gold-standard methods. These studies usually provide good recommendations in regards to which methods should be used, and which should be avoided.

From Papers I to III a series of different methods were used, from MMFF94 (a molecular mechanics model) to the more sophisticated ωB97X-D3BJ (hybrid DFT). The general objective was to use low levels of theory for initial geometry screening and high levels of theory for the final single-point energy calculations. The specific

details about which levels of theory were used can be found in the papers.

3.5.2 Geometry selection and optimization

One of the first steps in any molecular modeling experiment is the creation of an initial geometry, which will be a starting point for the next optimization steps. For that, a low level of theory method can be used to optimize a drawn structure. In this thesis work, the Avogadro software [87] was used to draw and optimize the initial ion pair conformers at the MMFF94 [88] level. At this point, either a manual or automated conformer search procedure was performed (since as previously explained, protic ionic liquids can exhibit several different low-energy conformers, and we should always attempt to find the lowest energy conformer possible to represent the bulk). In the case of the work from Paper I, a series of conformers were manually generated using this level of theory, which were further optimized using the semi-empirical method PM3 [89] in the Orca software [90]. The two lowest energy conformers at the PM3 level were further optimized at the Hartree-Fock level as well as at the B3LYP-D3 [91–94] level. Finally, the lowest energy conformer of the two was optimized using ωB97X-D3BJ [95].[17]

Although this procedure resulted in reasonable structures, automation could be used to explore even more conformers. Hence, in Paper III, the CREST software [96] was used to perform automated conformer searches. This software is capable of constructing, optimizing, and performing energy calculations in a large number (thousands) of geometries/conformers using excellent tight-binding semi-empirical methods (GFNn-xTB family of methods [97]).[18] At the end of this conformer search, the top 10 lowest energy conformers were further optimized using the r_2SCAN-3c functional [98] (which even outperforms some popular DFT functionals at a fraction of the computational cost). The lowest energy of these conformers was selected for a final single point energy calculation at the ωB97M-V level [99], which was used to calculate all the CDFT descriptors presented in Paper III. This automated procedure is not only easier to conduct, but much more comprehensive and thorough compared to manually selecting conformers, resulting in a much less biased conformer selection. Other important considerations in the selection of conformers are the choice of solvation models, dispersion corrections, and performing vibrational frequency analysis. As previously discussed, solvation effects are important in the modeling of protic ionic liquids, therefore, a few different solvation models were used. For the CREST calculations, acetone implicit solvation using the GBSA model [97, 100] was used. For the DFT calculations, ethanol implicit solvation

17: In retrospect, using five different levels of theory is certainly not necessary to achieve good results. For example, the use of Hartree-Fock and B3LYP-D3 was certainly not detrimental to the work, but could have been avoided, resulting in similarly good final results.

18: To put this improvement into perspective, this level of theory (specifically GFN2-xTB [97]) is significantly more accurate than PM3 (which was used in Paper I) while having a fraction of the cost. Furthermore, in my opinion, GFN2-xTB is likely to perform better than some very popular DFT functionals commonly used in the literature.

using the CPCM model [101] was used. These solvation models are by no means perfect representations of the solvation effects of other ionic liquid molecules, but can significantly improve the results of the calculations [102]. Dispersion corrections are also essential in these systems [103], since these forces dictate much of the behavior of ionic liquids (apart from the very strong Coulombic interactions). Finally, vibrational analysis must be performed to exclude the possibility of these conformers being in a transition state (since transition states will exhibit so-called imaginary vibrational modes).

3.5.3 Analysis of the computational results

A lot of information about the molecular modeling experiments can be extracted from the Orca output files (.out), like HOMO/LUMO energies, single-point energies (total electronic energy of the system), partial atomic charges, and vibrational frequencies. CDFT descriptors can be calculated from the HOMO/LUMO energies using Equations 2.2, 2.3 and 2.4. These are only some of the pieces of information that are immediately available after the calculation is over, but a lot more can be done with the output files. For instance, the Avogadro software [87] can be used to measure bond lengths, observe animated vibrational modes,[19] plot infrared simulated spectra and much more. Electrostatic potential maps, which can be used to spot differences in the electrostatic potential (which can be interpreted as being related to charge distribution) of the molecule, were calculated using the Gabedit software (using the .wfn/.wfx files from Orca as input) [105]. Finally, the MultiWFN [60] software can be used for a number of different electronic analyses (normally with the .wfn/.wfx files as inputs). In the case of Paper II, it was used to calculate hydrogen bonding strengths [61], based on AIM theory [63].

19: In this context, another valuable software is called vibAnalysis [104]. It was used to aid in the assignment of vibrational modes to the experimental FTIR spectra presented in Paper I. This software allows for a less subjective analysis of these vibrational modes, since it provides a list of all vibrational frequencies and a description of the most prominent displacements.

Results and discussion 4

4.1 Challenges on the synthesis of the bases

As discussed in the previous sections, before making any ionic liquid, we needed decent amounts (up to 20 g) of pure (98+%) and dry (under 1000 ppm) bases. All were synthesized using the same alkylation reaction (Figures 4.1 and 4.3), but each synthesis presented a unique set of challenges, which will be discussed in the next sections. More experimental details on these syntheses can be found in Papers I and III.

4.1.1 Triazole bases

Our first research project, which resulted in the publishing of Paper I, had as a first objective the synthesis of 1-ethyl-1,2,4-triazole. Triazole is an interesting analog to imidazole, which has been explored by other groups before [35], so we thought that it would be interesting to see if viable (with interesting properties for the intended application) protic ionic liquids could be made from triazole and how their properties would change in relation to their imidazolium counterparts. Our first attempt to synthesize 1-ethyl-1,2,4-triazole was based on the work by Alpers et al. [106], which described the synthesis of 1-ethyl-1,2,4-triazole as well as a series of other triazole compounds. Although this attempt was successful at producing 1-ethyl-1,2,4-triazole (verified by ^{1}H- and ^{13}C-NMR spectra, see Figure 4.2), it also produced the dialkylated side product (third product from top to bottom of Figure 4.1), which significantly reduced the yield of the reaction. This probably happened since the original procedure required a ratio of 1,2,4-triazole to 1-iodoethane of 1:2 (probably with the intention of increasing the yield) and a fairly small volume of solvent (10 mL of acetone per gram of 1,2,4-triazole). This resulted in a high concentration of alkylating reagent, which promotes dialkylation.

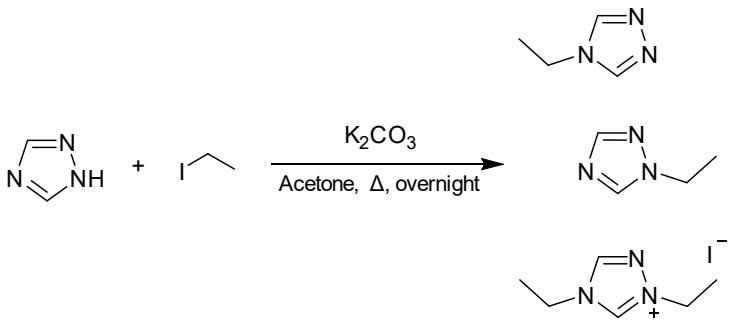

Figure 4.1: Synthesis scheme of the alkylation of 1,2,4-triazole with 1-iodoethane. This scheme shows some of the possible products from this synthesis.

This issue was resolved by decreasing the amount of alkylating reagent (ratio of 1:1.2), which worked even with a reduced amount of solvent (half of the original amount). Additionally, in the reference paper, the final crude product was distilled only once, which we deemed to be insufficient for achieving high purity. Therefore, our product was distilled twice, as well as treated with activated charcoal and molecular sieves to remove colored impurities and water. This resulted in a dry final product with a purity of 98.8% (assay by GC). Another concern that needed to be addressed was the possibility of the product being either a mixture of both alkylation products (1-ethyl-1,2,4-triazole and 4-ethyl-1,2,4-triazole) or not the isomer we were expecting (1-ethyl-1,2,4-triazole). These possibilities were quickly dismissed by analyzing the ^{1}H-NMR data for the purified product, since the product presented two singlets (integrating for two hydrogens) in the aromatic region (around 8 ppm), while 4-ethyl-1,2,4-triazole should present only one since both ring hydrogens are equivalent (first product from top to bottom of Figure 4.1). This result was further confirmed by analyzing the ^{13}C-NMR spectrum of the product as well as by comparing both experimental with simulated spectra.

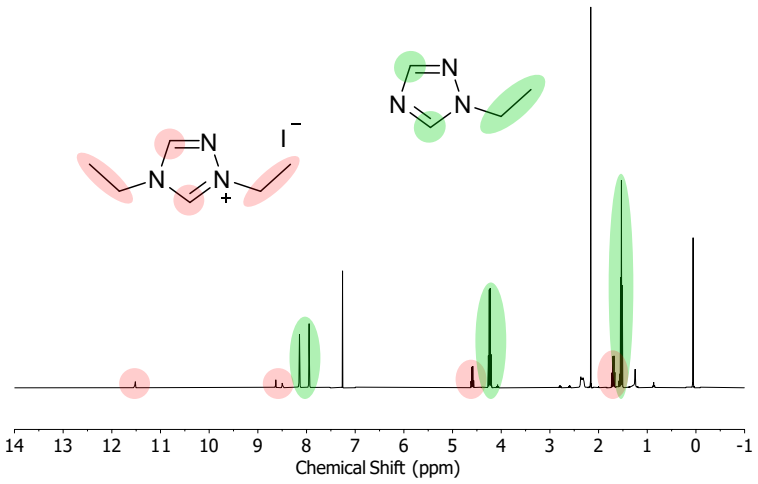

Figure 4.2: ^{1}H-NMR spectrum of the crude product from the first alkylation of 1,2,4-triazole with 1-iodoethane. Red markers show the peaks related to the dialkylated side product, while green ones mark the desired product.

4.1.2 Nitro- and cyano-functionalized imidazole bases

The initial objective of this project (which resulted in Paper III) was to make ethylated nitro- and cyano-functionalized imidazole bases,[1] so that their corresponding ionic liquids could be compared with the ones investigated in Paper I. We were successful in synthesizing 1-ethyl-4,5-dicyanoimidazole (up to approximately 10 g of product) after a few modifications compared to the synthesis of 1-ethyl-1,2,4-triazole (changing the solvent from acetone to acetonitrile and purifying the product by recrystallization in

1: The objective of this functionalization was to increase cation acidity [107], which could be beneficial in fuel cell systems [11, 12].

water). Motivated by the success of this reaction, we decided to move to the ethylation of 4-nitroimidazole. This, however, proved to be a much more challenging synthesis. It is easy to see why this is the case by just looking at the possible products, compared to the alkylation of 4,5-dicyanoimidazole (Figure 4.3).

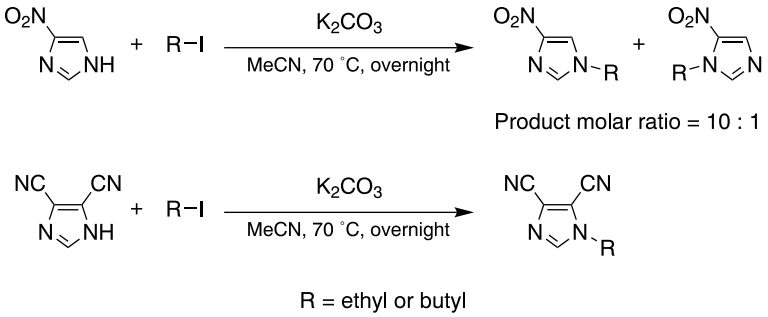

Figure 4.3: Synthesis scheme of the alkylation of 4-nitroimidazole and 4,5-dicyanoimidazole. This scheme shows the conditions used in the final optimized large batch reactions.

Since 4,5-dicyanoimidazole is somewhat symmetrical,[2] the electrophilic attack by a single molecule of the alkylating agent will result in one product only. However, that is not the case for 4-nitroimidazole, which can form two different products (also forming the dialkylated compound). During the first small-scale trial reactions, we noticed that the ratio between the main product and the side product was close to 10:1 (as estimated from the integration of the aromatic peaks in the ^{1}H-NMR spectrum of the crude product, see Figure 4.4).

2: In the sense that it can tautomerize by exchanging a hydrogen between the ring nitrogens

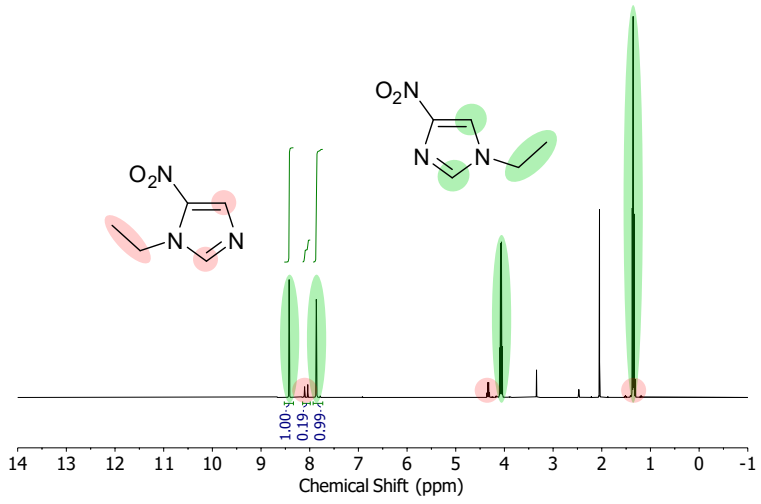

Figure 4.4: ^{1}H-NMR spectrum of the crude product from one of the first alkylation reactions of 4-nitroimidazole with 1-iodoethane. Red markers show the peaks related to the regioisomer side product, while green ones mark the desired product.

A series of trial experiments were performed trying to adjust this ratio and increase the selectivity of the main product,[3] but consistently failed to affect the ratio between the isomers. Since we couldn't increase the selectivity of the reaction, our next option was to develop a separation method. Unfortunately, that was not simple at all, since both isomers are very similar, meaning that their physicochemical properties are very similar as well. We attempted to separate these compounds by distillation, but

3: We tried changing the amount of alkylating agent, amount and type of solvent, changing the temperature, trying a different alkylation reagent, modifying the rate of addition of the alkylating agent, and other variations.

thermal decomposition started at the distillation temperature. We were still able to collect a small amount of clear liquid from this trial distillation, which by NMR analysis we determined to be a mixture of both isomers, though with the minor product in a higher concentration. That gave us the idea to modify the structure of the base in an attempt to change its physical properties (hopefully boiling point), and help with the separation.[4] After some optimization of the butylation reaction (changing the solvent from acetone to acetonitrile and increasing the reaction temperature from 40 to 70 °C, in order to increase the yield), we managed to get a crude product that could be purified by distillation. Multiple rounds of distillation were still required to get a final product that wasn't highly colored (the first distillation resulted in a dark orange liquid[5] that crystallized upon cooling). At the end of these multiple distillations, the final product (1-butyl-4-nitroimidazole) was an off-white solid with only trace amounts of the side product being detected by ^{1}H-NMR (99.8% purity by GC).

At that point, our next task was the synthesis of 1-butyl-4,5-dicyanoimidazole, which thankfully was quite easy. The compound was synthesized using the same conditions as in the butylation of 4-nitroimidazole, resulting in a crude pale yellow liquid (after a solvent extraction step) that was easily distilled into a clear off-white liquid (99.8% purity by GC).

4: We were also hoping that by increasing the alkyl chain length the selectivity would change, since the larger butyl chain might prefer to attack the least sterically hindered nitrogen (the one on the opposite side of the nitro group). This however, did not happen, since the ratio between products was almost the same as the one in the ethylation reaction.

5: The orange coloration was a result of the freshly distilled product being thermally degraded during the distillation, which is a problem unique to the Kugelrohr apparatus used for these distillations (since the product was condensing inside the oven, meaning that it was still experiencing high temperatures after condensation). This could potentially be avoided by using a traditional short-path distillation setup.

4.2 Challenges in the synthesis of the protic ionic liquids

Figure 4.5 shows our first setup used to synthesize protic ionic liquids. This first prototype was built with the objective of constructing a setup that would take into consideration all of the concerns and constraints discussed in this thesis and in Paper I (1:1 acid-to-base ratio, corrosion, no impurities, etc.). The idea was to use the ionic liquid that was just synthesized as a type of solvent to clean the addition funnel of any remaining acid traces, avoiding the use of any solvents. This setup was filled up inside the glovebox and transported (sealed) to a Schlenk line, where it was connected to a nitrogen gas line. The freshly made ionic liquid was recirculated using a peristaltic pump, with chemically resistant tubing. Although the fundamental idea was good (and it was quite fun to build and see working), it was too complicated and impractical. However, this prototype gave me the inspiration and insight required to build the setup later used in Papers I and III.

Figure 4.5: First prototype of a protic ionic liquid synthesis setup. This setup, uses a peristaltic pump to recirculate the protic ionic liquid from the bottom to the top of the system.

4.2.1 Triazolium- and imidazolium-based protic ionic liquids

The setup described in Paper I was well-suited to make the triazolium- and imidazolium-based[6] protic ionic liquids (Figure 4.6). Both precursor bases are liquids, which means that there was always at least one precursor (acid or base) that was a liquid. Also, the ionic liquids produced had fairly low viscosities, meaning that they could be easily recirculated using the syringe, which was necessary to ensure that all acid measured reacted with all of the base measured. Although we were able to successfully use this setup to make pure (98–99% m/m purity by quantitative ^{19}F-NMR) and dry (128–553 ppm of water by KF titration) protic ionic liquids, having to remove the entire setup (see Figure 3.2) from the glovebox for cooling was a clear limitation, as previously discussed in the Methods chapter.

6: Both imidazolium-based protic ionic liquids studied in Paper I were commercially available, however, the [C_2HIm][TFSI] sample we purchased from IoLiTec was too impure (approximately 94% purity according to our own ^{1}H-NMR purity essay), hence we decided to make our own. The only protic ionic liquid that was not synthesized was [C_2HIm][TfO], since the IoLiTec sample was deemed to be pure enough (>99%).

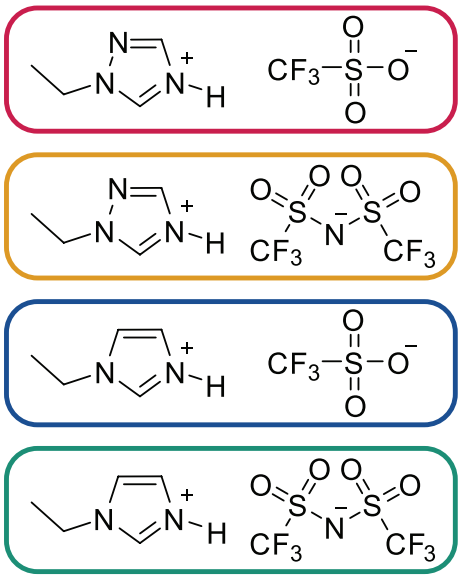

Figure 4.6: Molecular structure and color coding of all the protic ionic liquids considered in Paper I and II. From top to bottom: $[C_2HTr_{124}][TfO]$, $[C_2HTr_{124}][TFSI]$, $[C_2HIm][TfO]$ and $[C_2HIm][TFSI]$. This color coding is valid for data from Paper I and II only.

4.2.2 Nitro- and cyano-functionalized imidazolium protic ionic liquids

The synthesis of nitro- and cyano-functionalized imidazolium protic ionic liquids (Figure 4.7) was performed in a similar way compared to the one previously discussed,[7] with one of the main differences being the use of the Polar Bear Plus instrument.

By using this instrument, cooling and heating could be performed inside the glovebox,[8] eliminating the need to remove the setup from the glovebox. Another important modification was the use of a solvent, since one of the bases (1-butyl-4-nitroimidazole) is a solid. Another difficulty we faced with one of these syntheses, was the high viscosity of $[C_4H-4,5-(CN)_2Im][TFSI]$, which made the recirculating step impossible. To deal with that, the temperature of the product was raised to 60 °C, which significantly reduced its viscosity, making it possible to manipulate it with the syringe. Since both of these ionic liquids were highly viscous, in order to manipulate them (for the preparation of samples, etc.), this same heating procedure was performed. Finally, it is important to mention that we attempted to synthesize TfO-based protic ionic liquids (by using triflic acid to neutralize the bases), however, we were unsuccessful. During the addition of the HTfO acid to the bases, solid products formed (even before the entire amount of acid had been added), which appeared to have high melting points (above 80°C most likely). Because of the formation of a solid product, our synthesis setup is unsuited for the synthesis of these types of compounds, unless a solvent is used. We believe that even if a solvent was used and a 1:1 ratio between acid and base was properly achieved, the final product was likely to have a high melting point, which is not suitable for our intended application.

7: $[C_4HIm][TFSI]$ was purchased from IoLiTec and served as a reference for an unmodified imidazolium-based protic ionic liquid.

8: The Polar Bear Plus instrument can only work if the surrounding temperature is below 34 °C, meaning that the temperature inside the glovebox has to be kept low. Since the volume of the glovebox is quite small, the interior temperature can rise quite significantly simply by operating this instrument for an extended period of time, but the main source of heat inside the glovebox is the heat from the gas inlet (hot nitrogen gas coming from the glovebox regeneration system). Thankfully, there are many ways to deal with this problem (like air-conditioning systems, or intake gas water coolers). In our case, keeping the doors of the lab open and cooling the glovebox with wet paper towels did the trick!

Hence, we decided to only make TFSI-based compounds and not further investigate the TfO-based counterparts.

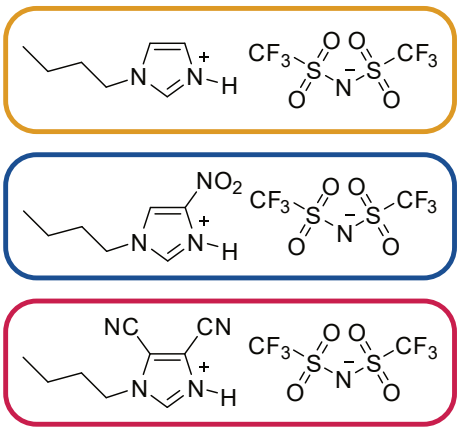

Figure 4.7: Molecular structure and color coding of all the protic ionic liquids considered in Paper III. From top to bottom: $[C_4HIm][TFSI]$, $[C_4H-4\text{-}NO_2Im][TFSI]$ and $[C_4H-4,5-(CN)_2Im][TFSI]$. This color coding is valid for data from Paper III only.

4.3 Differences in acidity

4.3.1 Experimental evidence for increased acidity

To confirm the structure of all ionic liquids synthesized in this thesis work, qualitative ^{1}H-NMR (as well as ^{13}C- and ^{19}F-NMR) was performed, using pure samples inside coaxial NMR tubes (Figure 3.3). This was done to analyze the chemical shifts of our species without the influence of atmospheric moisture and a solvent (since the DMSO-d_6 is contained inside the inner coaxial capillary tube). This NMR analysis not only confirmed that the structures of the ionic liquids were as expected, but also gave us the first indication that they have different Brønsted acidities.

Before looking at the experimental data, let us discuss my hypothesis[9] for how the acidity of protic ionic liquids might be related to the chemical shift of the NH hydrogen. The chemical shifts of different nuclei are related to their electronic environment. Hydrogens around groups that donate electron density will be shielded, while hydrogens in electron-poor environments will be deshielded, and hence, will have a higher chemical shift. Electron-withdrawing groups around hydrogen will pull electron density (deshielding them, pushing their shifts to higher values, i.e. downfield), which will also increase their acidity through the inductive effect. Hence, this is the logic behind the claims about the effects of cation structure on the acidity of the N-H bond. Another factor that can influence the chemical shift of these hydrogens is the structure of the anion. Anions that form strong hydrogen bonds with the cation (in the case of these protic ionic liquids the strongest hydrogen bond is normally the one with the NH hydrogen), will draw a hydrogen from the cation closer to them, deshielding it due to the

9: Here, I mean that this needs to be further verified by more studies on these systems.

weakening of the covalent bond between the hydrogen and the cation. This means that strong hydrogen-bonding anions will cause these protons to shift downfield, while weak hydrogen-bonding anions will cause an upfield shift.[10] This effect has been shown by studies in both protic [108] and aprotic [109] ionic liquids. in Paper I, I made the argument that this weakening of the N-H covalent bond by stronger hydrogen bonding increases the Brønsted acidity of the cation. This logic is behind the claims regarding differences in acidity due to anion selection. However, I now believe that this might be wrong. Although the N-H bond will stretch in response to a higher degree of hydrogen bonding, this hydrogen is still strongly bonded to the entirety of the ion pair, meaning that it's not willing to leave the ion pair and protonate a third molecular species (i.e. lower acidity due to a higher degree of hydrogen bonding). This can be seen by comparing the Hammett acidity[11] (H_0) of acidic protic ionic liquids with different anions but the same cation, with anions like BF_4^- and TfO^- displaying lower H_0 values (high acidity) while strongly coordinating anions like CH_3COO^- display higher values (low acidity) [112, 113].

10: Other effects can cause changes in the hydrogen's shielding, hence, not all differences in chemical shift should be attributed to changes in the position of the hydrogen. Therefore, I argue that the chemical shift of hydrogens should not be used as the only descriptor of acidity, but used in conjunction with other descriptors, in order to provide a better assessment of the differences in acidity between compounds.

11: The Hammett acidity function can be used to determine the relative acidity of different ionic liquids, by probing their interactions with a third molecule (usually a nitroaniline compound) by UV/vis spectroscopy [110, 111].

With this in mind, we can now analyze the Qualitative ^{1}H-NMR of the pure (no solvent) protic ionic liquids from Paper I (Figure 4.8) and III (Figure 4.9).

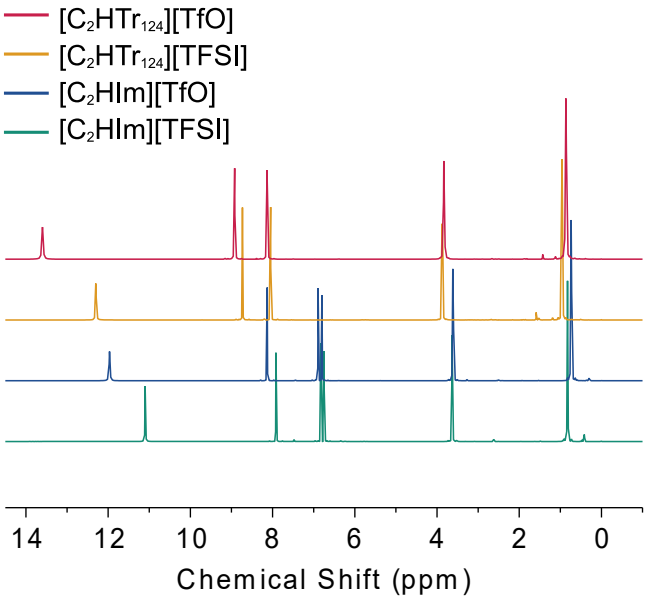

Figure 4.8: Qualitative ^{1}H-NMR of all ionic liquids from Paper I.

If we look at the NH peaks (singlets in the range of 14-10 ppm) of all ionic liquids from Paper I, a clear difference in the chemical shifts can be seen when comparing two ionic liquids with the same anion (e.g. $[C_2HTr_{124}][TfO]$ and $[C_2HIm][TfO]$, or $[C_2HTr_{124}][TFSI]$ and $[C_2HIm][TFSI]$). The same can be observed for the ring hydrogens (peaks in the range of 9-6 ppm). This difference in chemical shifts can also be observed in the ionic liquids from Paper III (Figure 4.9).

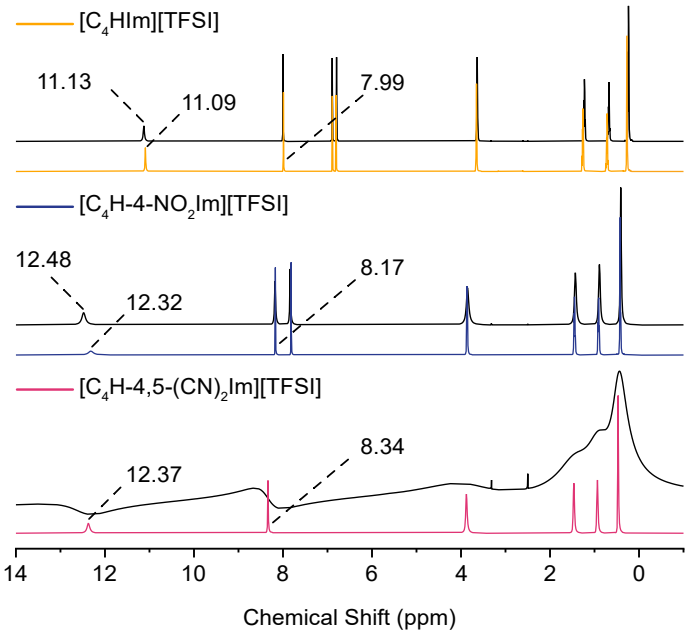

Figure 4.9: Qualitative ^{1}H-NMR spectra of all ionic liquids from Paper III, recorded at two different temperatures (black lines for 25 °C and colored lines for 60 °C).

Whereas the NH peak for the unmodified [C_4HIm][TFSI] can be observed at 11.09 ppm (at 60 °C[12]), the functionalized ionic liquids [C_4H−4-NO_2Im][TFSI] and [C_4H−4,5−$(CN)_2$Im][TFSI] presented shifts with higher values (12.32 and 12.37 ppm respectively). This was the first indication of higher acidity from experimental data and will be further explored in the next sections. Additionally, it will be compared with other experimental results, as well as data from molecular modeling experiments.

12: In order to reduce the viscosity of the protic ionic liquids, the spectra were collected at 60 °C (and compared with the less resolved, broader spectra at 25 °C).

Another indication of the higher acidity of triazolium-based protic ionic liquids comes from their FTIR spectra (Figure 4.10).

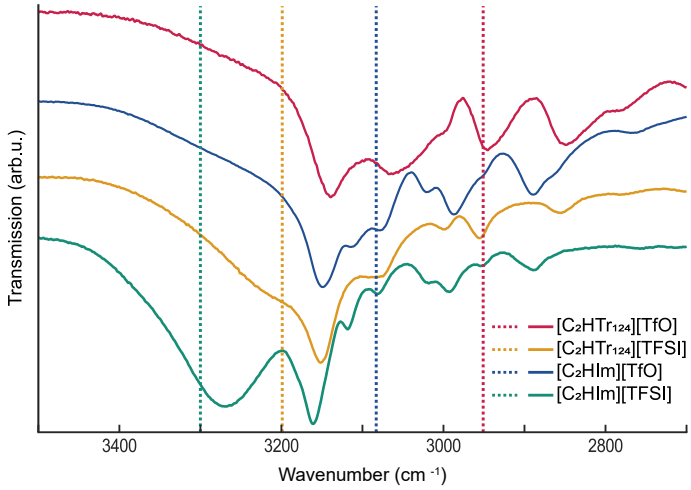

Figure 4.10: Experimentally recorded FTIR spectra (vertically offset for clarity), of all ionic liquids from Paper I, in the frequency region of the N-H and C-H stretching modes. Dashed lines correspond to the calculated frequencies for the N-H stretching.

The region of the N-H stretching mode (between 3400 and 2900 cm^{-1}) can provide some additional information regarding the relative acidity of these compounds. Stretching modes at higher frequencies usually indicate higher bonding strength between the atoms involved in the bond, as determined by modeling these

vibrational modes using Hooke's law.[13] By describing these vibrational modes as classical harmonic oscillators, we can see that the frequency of the vibrational modes is directly related to the force constant (bond strength) of the "spring" formed by two atoms, hence, higher frequency vibrations are related to stronger bonds. In the context of Brønsted acidity, higher bonding strength means lower acidity, therefore, the higher the vibrational frequency of an N-H bond is, the lower its acidity will be.

13: Hooke's law for a classical harmonic oscillator ($\tilde{\nu} = \frac{1}{2\pi c}\sqrt{\frac{k}{\mu}}$). k is the force constant (or spring constant), μ is the reduced mass and c is the speed of light [75].

By analyzing the FTIR of the ionic liquids in Paper I (Figure 4.10) using this logic, it becomes clear that triazolium-based protic ionic liquids must be more acidic (in agreement with the ^{1}H-NMR results) compared to imidazolium compounds. If we look at the spectrum of [C_2HIm][TFSI], we can see a broad band at 3271 cm^{-1}, which corresponds to the N-H vibrational mode. This band should be present in all other protic ionic liquids, but it appears to be shifting to lower vibrational frequencies from the lower spectrum ([C_2HIm][TFSI]) to second from the bottom ([C_2HTr$_{124}$][TFSI]), indicating that the change from imidazolium to triazolium causes this shift.[14] More on this analysis from the perspective of computational chemistry calculations will be discussed in the next section. The same type of shift can be seen in the FTIR spectra of the compounds from Paper III (Figure 4.11).

14: This same analysis was inconclusive in the case of TfO-based compounds, since the N-H peaks seem to be very broad and lower in intensity. They are also overlapping with other peaks in the region.

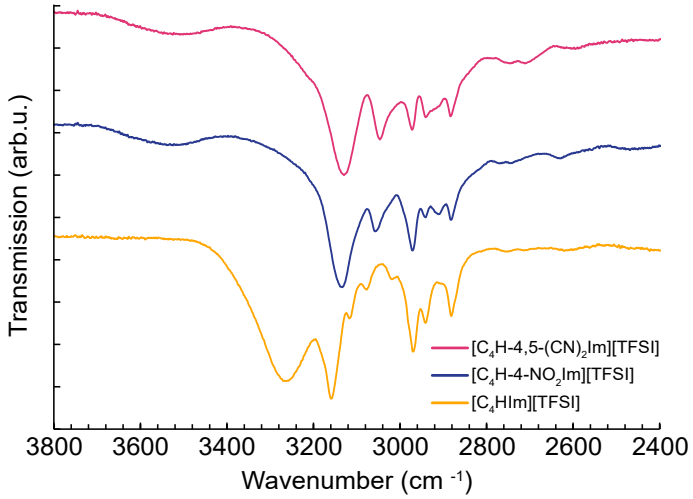

Figure 4.11: Experimentally recorded FTIR spectra (vertically offset for clarity), of all ionic liquids from Paper III, in the frequency region of the N-H and C-H stretching modes.

Here, we can clearly see the effect of these electron-withdrawing groups on the electronic structure of the imidazolium ring, since the peak at 3263 cm^{-1} appears to have shifted to lower frequencies (combining with the peaks in the center of the spectra, as evidenced by the increased area under the curves).

All of these experiments seem to indicate the same, that by pulling electron density from the N-H bond,[15] it's acidity will increase. This is a well-known effect, being described in many organic chemistry books for other classes of organic compounds. Finally, the effect of the anion on the acidity cannot be conclusively determined by

15: Either by changing a carbon in the ring by a more electronegative atom like nitrogen (changing from imidazole to triazole), or by adding NO_2 or CN groups to the imidazolium ring.

these experimental methods, which will be discussed in the next sections.

4.3.2 Computational insights on the increased acidity

Although the electron-withdrawing effect of a nitro group (or cyano) is quite well known [107], the effect of having an extra nitrogen in the cation ring (as is the case of triazolium as compared to imidazolium) is not as obvious. To clearly see this effect, we can look at the electrostatic potential map for two protic ionic liquids from Paper I, i.e., $[C_2HTr_{1,2,4}][TfO]$ and $[C_2HIm][TfO]$ (Figure 4.12).

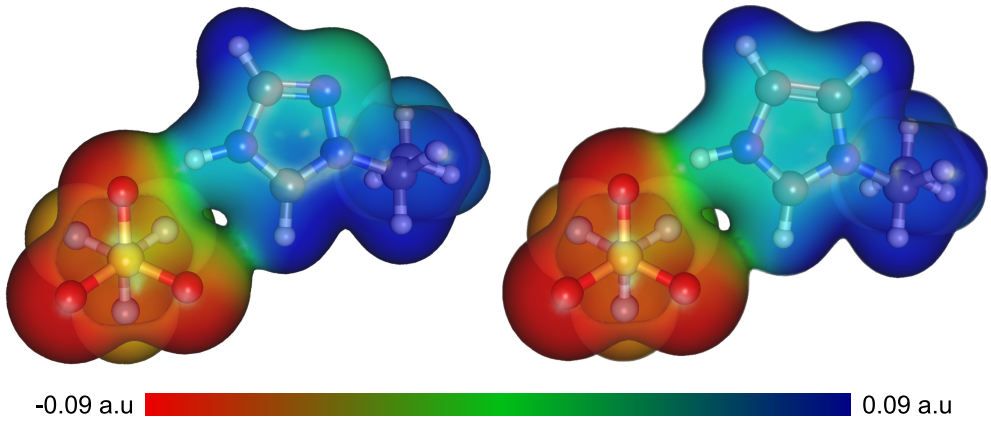

Figure 4.12: Electrostatic potential map (plotted on the electron density isosurface with a value of 0.007) for the $[C_2HTr_{1,2,4}][TfO]$ and $[C_2HIm][TfO]$ optimized ion pairs in the ωB97X-D3BJ/cc-pVTZ/CPCM(Ethanol) level of theory.

There is a clear change in the electrostatic potential when comparing $[C_2HIm][TfO]$ (on the right) to $[C_2HTr_{1,2,4}][TfO]$ (on the left). If we substitute a CH for a N, electron density will start moving towards that region of the ring, meaning that it will move away from the N-H bond, making it more acidic.[16] Bond polarization is a clear indicator of acidity, with bonds that are highly polarized being generally more acidic. One way of determining this polarization, is to calculate the partial charges for the nitrogen and hydrogen in the N-H bond using the CHELPG scheme (Figure 4.13).

16: Although this electrostatic potential map was not calculated for the ionic liquids in Paper III, a similar effect should be present, where the nitro and cyano groups would accumulate electronic density.

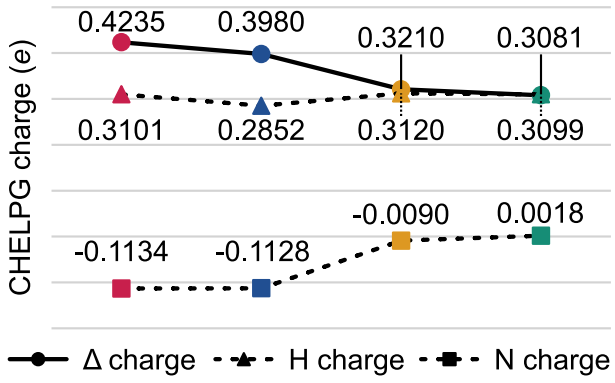

Figure 4.13: Partial atomic charges (CHELPG scheme) for all the optimized ionic liquid ion pairs from Paper I in the ωB97X-D3BJ/cc-pVTZ/CPCM(Ethanol) level of theory. From left to right respectively: $[C_2HTr_{1,2,4}][TfO]$, $[C_2HIm][TfO]$, $[C_2HTr_{1,2,4}][TFSI]$ and $[C_2HIm][TFSI]$.

If we analyze the CHELPG data for the two ionic liquids from Figure 4.12, we can see that [$C_2HTr_{1,2,4}$][TfO] has a higher Δ charge (absolute difference in charges between the N and H atoms in the N-H bond) of 0.4235 *e* compared to 0.3980 *e* for [C_2HIm][TfO]. The same trend can be observed for the TFSI-based compounds. N-H bond length (Table 4.1) is another descriptor of Brønsted acidity. The lengthening of a bond is an indication of decreased bonding strength, which in the case of these N-H bonds, can indicate higher acidity.

Table 4.1: Selected bonds and interatomic lengths (Å) for all the optimized ionic liquid ion pairs from Paper I in the ωB97X-D3BJ/cc-pVTZ/CPCM(Ethanol) level of theory.

Protic ionic liquid	N – H	(N)H···O^{anion}	N(H)···· O^{anion}
[$C_2HTr_{1,2,4}$][TfO]	1.038	1.708	2.738
[$C_2HTr_{1,2,4}$][TFSI]	1.025	1.858	2.882
[C_2HIm][TfO]	1.031	1.763	2.787
[C_2HIm][TFSI]	1.019	1.950	2.959

By comparing the N-H bond lengths of imidazolium- and triazolium-based protic ionic liquids, a clear lengthening of the bonds can be observed. For example, while the N-H bond in [C_2HIm][TfO] is 1.031 Å, the one in the triazolium counterpart is 1.038. The same lengthening can be observed for the TFSI-based compounds. The differences in electronic structure also have an effect on the hydrogen bonding length, but this will be discussed in the context of the changes in transport properties in a subsequent section. These changes in the N-H bond lengths were also reflected in the predicted N-H vibrational mode frequencies, as displayed by the dashed lines in Figure 4.10.[17] Another way of comparing the acidity of molecules is by the use of CDFT descriptors, like electrophilicity and electronegativity, which are derived from HOMO/LUMO energy calculations. These properties relate to the ability of a molecular system to attract and accept electrons, which means that they are measurements of Lewis acidity [114, 115]. Brønsted acidity has been demonstrated to generally (but not always) follow Lewis acidity [59], for a series of different compounds, therefore, electrophilicity[18] and electronegativity might be considered to be indicators of Brønsted acidity as well. Interestingly, in my experience, these descriptors appear not to be strongly affected by small changes in the geometry of the molecule, which means that they are somewhat robust when compared to other descriptors that are very dependent on geometry (CHELPG charges, bond lengths, and N-H vibrational frequency).[19] With that in mind, we can now analyze the calculated CDFT descriptors for the protic ionic liquids in Paper I (Table 4.2) and III (Table 4.3).

Once again, there are indications that triazolium-based protic ionic liquids are more acidic compared to imidazolium counterparts. The triazolium compounds consistently present higher electronegativities and electrophilicities. These results also seem

17: Importantly, these vibrational modes tend to be poorly estimated by this type of DFT calculation, since these are highly sensitive to their chemical environment, which is not appropriately modeled by single ion pair computational experiments. More about this will be discussed in the Conclusions and outlook chapter.

18: Electrophilicity could even be interpreted as electronegativity scaled by hardness.

19: An extended discussion on this can be found in the Conclusions and outlook chapter.

Protic ionic liquid	Eletronegativity (eV)	Electrophilicity (eV)
$[C_2HTr_{1,2,4}][TfO]$	4.5839	1.7482
$[C_2HTr_{1,2,4}][TFSI]$	4.8269	1.8888
$[C_2HIm][TfO]$	4.1659	1.4525
$[C_2HIm][TFSI]$	4.2305	1.5052

Table 4.2: CDFT molecular descriptors for all the ionic liquid ion pairs in Paper I in the ωB97X-D3BJ/cc-pVTZ/CPCM(Ethanol) level of theory.

to indicate that TFSI-based ionic liquids should be slightly more acidic, which would be in line with the previous discussion about the effects of anion hydrogen bonding interactions on the acidity of protic ionic liquids. A similar trend was found on the nitro- and cyano-functionalized protic ionic liquids of Paper III.[20]

20: Keep in mind that these electrophilicity values cannot be compared between the two different Papers, since they were calculated using different levels of theory.

Protic ionic liquid	Eletronegativity (eV)	Electrophilicity (eV)
$[C_4HIm][TFSI]$	4.7085	2.0504
$[C_4H-4\text{-}NO_2Im][TFSI]$	5.9561	3.6593
$[C_4H-4,5-(CN)_2Im][TFSI]$	5.6943	3.2998

Table 4.3: CDFT molecular descriptors for all the ionic liquid ion pairs in Paper III in the ωB97M-V/def2-TZVPD/CPCM(Ethanol) level of theory.

The modification of the imidazole ring with nitro and cyano groups has a drastic effect on the acidity of these types of protic ionic liquids, as can be seen from the increase in the CDFT descriptors. While the CDFT descriptors predict that $[C_4H-4\text{-}NO_2Im][TFSI]$ should be more acidic than $[C_4H-4,5-(CN)_2Im][TFSI]$, we could not confirm this by analyzing the experimental data, meaning that additional experiments would have to be performed to confirm this prediction. The only clear result is that $[C_4HIm][TFSI]$ must be significantly less acidic compared to the other two ionic liquids from Paper III.

4.4 How does acidity affect the physicochemical properties of protic ionic liquids?

Changing the acidity of the cations will have an effect on the strength of the hydrogen bonding between the ions. Additionally, changing the anions will also affect hydrogen bonding, as previously discussed. These changes will affect the properties of these ionic liquids, since, apart from Coulombic interactions, hydrogen bonding is usually the strongest intermolecular interaction between ions in protic ionic liquids [116, 117]. Possible evidence for this increased interaction between cation and anion can be seen when analyzing the Raman spectra of triazolium- and imidazolium-based protic ionic liquids, presented in Paper II (Figure 4.14). The strongest Raman signatures in TfO- and TFSI-based ionic liquids are usually the signals associated with stretching modes from anion moieties (~742 cm^{-1} mode related to ν_s S-N-S and ν_s CF_3 in [TFSI], the mode at ~760 cm^{-1} related to ν_s CF_3 in [TfO], and the mode at ~1035 cm^{-1} related to ν_s SO_3 in [TfO][21]), and these modes have been shown to be sensitive to coordination strength

21: These modes are well known in the literature, and these assignments were also confirmed by the DFT predicted spectra, as presented in Paper I.

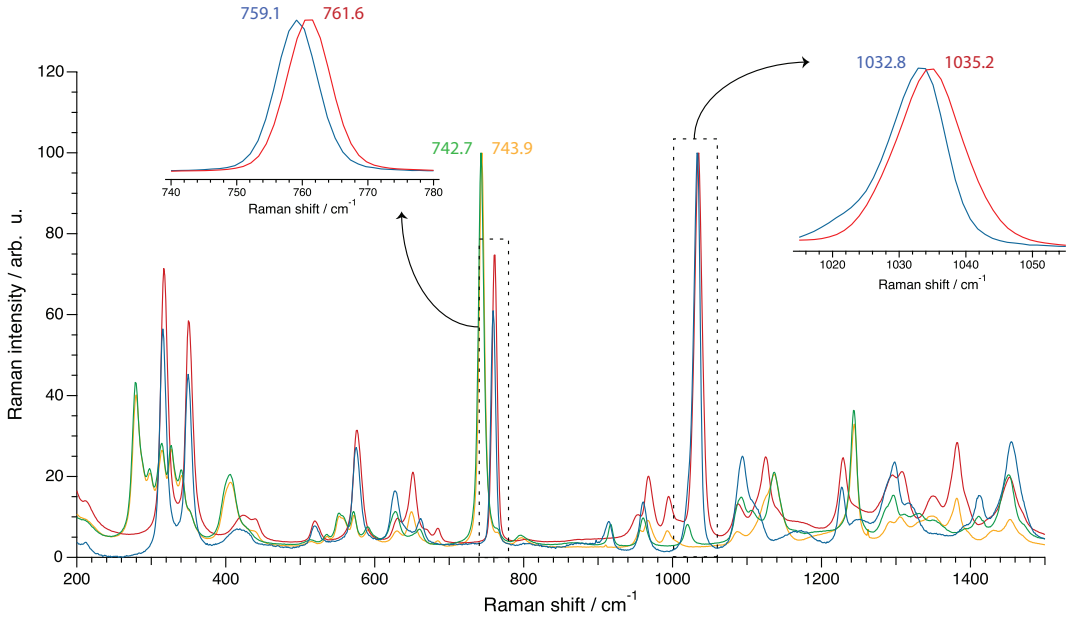

Figure 4.14: Raman spectra recorded at room temperature for all protic ionic liquids in Paper II, i.e., [C_2HIm][TFSI] (green), [C_2HTr$_{1,2,4}$][TFSI] (yellow), [C_2HIm][TfO] (blue) and [C_2HTr$_{1,2,4}$][TfO] (red). The insets (normalized) show zoomed-in regions to visualize relative frequency shifts of [TfO]-related vibrations.

22: This hypothesis was discussed in more detail in Paper II.

between [TFSI] and its counterion [118–121]. In short,[22] blue shifting (increase in Raman shift) of these frequencies should be associated with stronger intermolecular interactions between [TFSI]/[TfO] and their counterions. In Figure 4.14, we can see that changing the cation structure from imidazolium to triazolium has a small but measurable effect on the Raman shifts of these modes. Overall, these modes are blueshifting, indicating that triazolium-based protic ionic liquids have stronger intermolecular interactions (between cation and anion) when compared to imidazolium counterparts.

This increase in intermolecular interactions can also be seen when analyzing the hydrogen bond strengths (determined in the framework of QTAIM theory [63]) vs N-H length or hydrogen bond length (Figure 4.15). As the hydrogen bond length decreases, E_{HB} increases. This certainly makes sense, since this bond is being

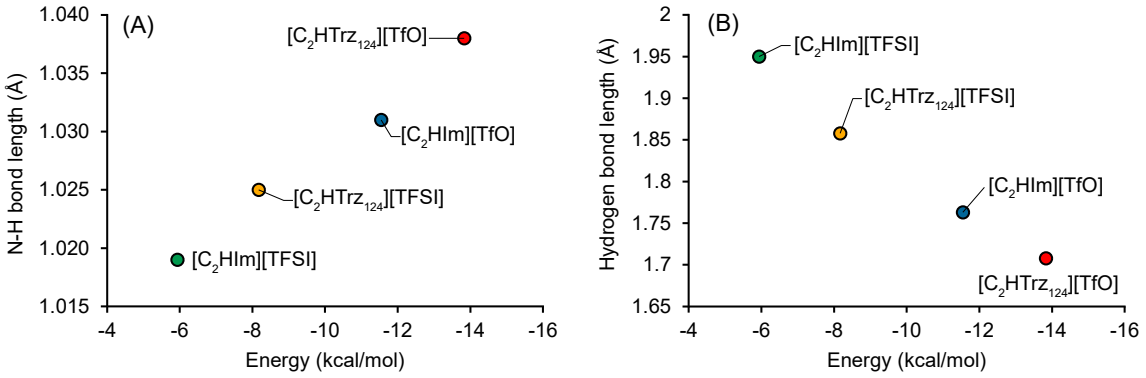

Figure 4.15: N-H bond length (**A**) and hydrogen bond length (**B**) as a function of hydrogen bonding energy (E_{HB}). Calculated at the ωB97X-D3BJ/cc-pVTZ/CPCM(Ethanol) level of theory.

shortened by the increasing interactions between cation and anion. The strength of this interaction increases from imidazolium- to triazolium- based compounds, as well as from [TFSI]- to [TfO]-based compounds. The higher coordination strength of [TfO] compared to [TFSI] is certainly nothing new, being reported many times in the literature. It is also clear that the elongation of the N-H bond is related to an increase in E_{HB}, which makes sense, since this type of interaction can be imagined as a tug-of-war between anion and cation, both pulling on the acidic N-H hydrogen. Overall, these results seem to indicate that switching the cation ring structure from imidazole to triazole will increase intermolecular interactions, likely, due to the increase in hydrogen bonding. The same can be said when going from [TfO]- to [TFSI]-based compounds, with [TfO] resulting in stronger interactions. The introduction of a nitro or cyano group to the imidazolium ring likely has the same effect of increasing hydrogen bonding.

Another characteristic of these ionic liquids that can be explained by the increased cation acidity is their thermal stability. It is well known that the thermal stability of protic ionic liquids is related to their ΔpK_a [122, 123]. Hence, increasing the acidity of the cation (which means reducing the basicity of the corresponding base) will decrease the ΔpK_a, and decrease the thermal stability. For instance, while imidazole has a pK_a of 18.6, 1,2,4-triazole has a pK_a of 14.8 [124]. The same reduction in pK_a is expected when adding electron-withdrawing groups to imidazole. These trends in thermal stability can be clearly seen in the TGA data from Paper I (Figure 4.16).

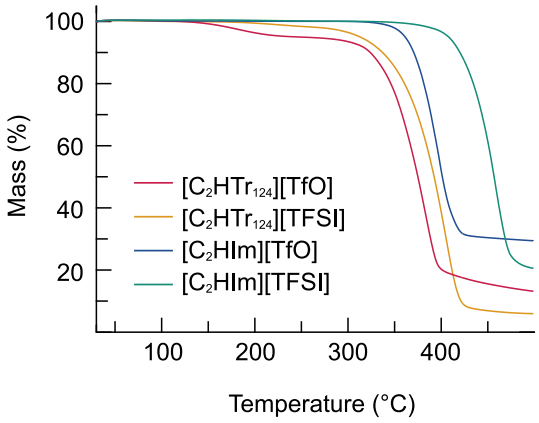

Figure 4.16: TGA curves of all protic ionic liquids from Paper I recorded under N_2 atmosphere, without heat treatment.

The most stable ionic liquid ([C_2HIm][TFSI]) is the one with the highest ΔpK_a, and the one with the lowest is the least stable ([$C_2HTr_{1,2,4}$][TfO]). Once again, if the acidity of the ionic liquid is high (meaning that the cation wants to donate a proton), back-proton transfer to the base is more likely to happen, forming more volatile neutral species, which reduces the thermal stability of the ionic liquid. The same can be seen for the ionic liquids from Paper III (Figure 4.17).

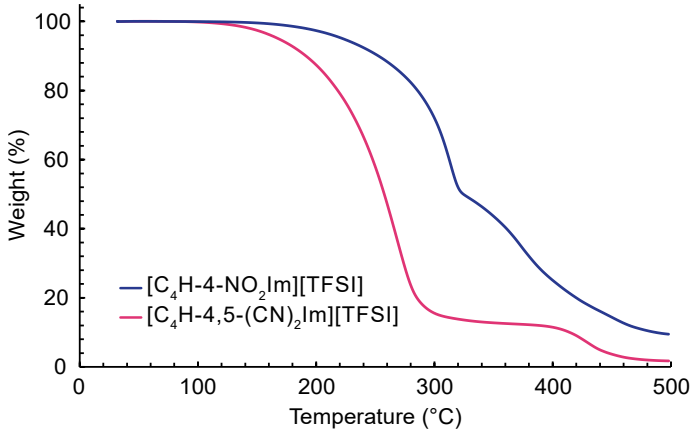

Figure 4.17: TGA curves of the nitro- and cyano-functionalized protic ionic liquids from Paper I recorded under N_2 atmosphere, without heat treatment.

Both functionalized protic ionic liquids, ([C_4H−4-NO_2Im][TFSI] and [C_4H−4,5−$(CN)_2$Im][TFSI]), show lower thermal stability when compared to the reported [125] T_d onset value (Table 4.4) for the unmodified compound ([C_4HIm][TFSI]), which is reasonable, since both of the modified cations are significantly more acidic due to the electron-withdrawing groups. The difference in thermal stability between the two functionalized protic ionic liquids likely cannot be explained simply by their difference in acidity, which is likely related to the thermal stability of the precursor bases. Importantly, although the thermal stability of protic ionic liquids is highly related to their ΔpK_a [122, 123], this is certainly not the only factor determining their stability, so other factors must be considered (like the thermal stability and boiling point of the precursor acid and base). The compiled data for all ionic liquids can be found in Table 4.4.[23]

23: When reporting TGA data, I believe it is important to present not only the T_d onset values but also T_d peak values as well as the full thermograph. Together, this data paints a more accurate picture of the behavior of these compounds.

Table 4.4: Onset and peak decomposition temperatures (estimated from TGA) for all ionic liquids in this thesis. The peak decomposition temperatures were determined from the first derivative of the TGA curves.

Protic ionic liquid	T_d onset (°C)	T_d peak (°C)
[C_2HTr$_{1,2,4}$][TfO]	343	383
[C_2HTr$_{1,2,4}$][TFSI]	358	406
[C_2HIm][TfO]	369	398
[C_2HIm][TFSI]	428	458
[C_4HIm][TFSI][1]	354	N/A
[C_4H−4-NO_2Im][TFSI]	280	314
[C_4H−4,5−$(CN)_2$Im][TFSI]	218	268

[1] For this ionic liquid, values have been taken from data already published in reference [125].

Finally, when interpreting this data, it is important to consider that these types of experiments are run over small periods of time and under an inert atmosphere. This means that the thermal stability reported by these kinds of experiments is not representative of the stability of these compounds under isothermal conditions. For instance, if the T_d onset temperature is 300 °C, it doesn't mean that the compound will suffer no decomposition before this temperature. Long-term isothermal TGA (at ambient air conditions) can be performed [126], but unfortunately, most researchers don't

have the resources to perform such type of analysis, since it requires using the TGA instrument for long periods of time.

The phase behavior of protic ionic liquids is also related to their acidity and the degree of coordination of the anion. The glass transition temperature is particularly relevant in the context of this thesis work, and although its dependence on intermolecular interactions is quite complicated [29], in general, stronger attractive intermolecular interactions tend to increase the T_g. Because of this, it is reasonable that hydrogen bonding will affect T_g [28]. It is also important to mention that T_g is notoriously sensitive to experimental conditions, so it should be analyzed carefully (at least under the same experimental conditions). The values of T_g for all ionic liquids in this thesis can be found in Table 4.5.

Protic ionic liquid	T_g (°C)
$[C_2HTr_{1,2,4}][TfO]$	-65.27
$[C_2HTr_{1,2,4}][TFSI]$	-61.60
$[C_2HIm][TfO]$[1]	N/A
$[C_2HIm][TFSI]$	-81.83
$[C_4HIm][TFSI]$[2]	-84
$[C_4H-4\text{-}NO_2Im][TFSI]$	-41.42
$[C_4H-4,5-(CN)_2Im][TFSI]$	-23.83

Table 4.5: Results from the thermal analysis by DSC of all protic ionic liquids in this thesis. Values are extracted from the 2nd cycle at a heating/cooling rate of 10 °C/min.

[1] This ionic liquid did not present T_g, instead presenting T_c and T_m at -18.26 and 22.27–29.11 °C respectively.

[2] For this ionic liquid, values have been taken from data already published in reference [125].

Overall, it appears that going from imidazolium- to triazolium-based protic ionic liquids, there is an increase in the T_g. The same increase is seen when functionalizing the imidazolium cation with electron-withdrawing groups. Interestingly, only $[C_2HIm][TfO]$ presented no glass transition, presenting crystallization and melting instead. Additionally, by using a slower cooling rate, crystallization and melting of $[C_2HIm][TFSI]$ could be detected, as well as a T_g (meaning that the compound formed crystalline and amorphous regions while cooling).[24] More discussions on the importance of these T_g values are presented in the next section.

24: It is important to comment that although no other transitions were detected for most ionic liquids in this thesis, it doesn't mean that they simply don't exist. Maybe by changing the experimental conditions (or even the purity of the ionic liquids), different transitions could be observed.

4.5 Rationalizing the differences in transport properties

Analyzing the transport properties of these compounds almost feels like putting together all the pieces of the puzzle, since these properties are dependent on all of the properties that we discussed so far. So first, let's discuss the most apparent transport property of these compounds, their viscosity.[25] Starting with the least viscous

25: Since no measurements were made on the viscosity of these compounds, this discussion is based on the visual examination of their fluidity.

ionic liquid in this thesis, [C_2HIm][TFSI]. By looking at all the data previously discussed, it becomes clear why its viscosity is so low. It is the least acidic cation, with a weakly coordinating anion, a small alkyl chain and it presents the lowest T_g. By switching the imidazole for triazole, there is a small but noticeable increase in the viscosity, likely due to the increase in acidity of the cation (stronger intermolecular interactions between the cation and anion). A significant increase in viscosity is seen when adding a nitro group to the imidazole ring, once again, likely due to the increase in acidity. Not only that, but the increase in the size of the cation (by using a butyl and a nitro group) clearly has an effect [127], as well as the increased possibility of π–π stacking introduced by the nitro group. Finally, the ionic liquid with the highest apparent viscosity is [C_4H−4,5−$(CN)_2$Im][TFSI] (which has a fluidity comparable with thick honey). This is once again quite expected, since it is the largest cation (with a rigid cation structure due to the linearity of the CN groups), one of the most acidic and with two groups capable of π–π stacking. This high viscosity can be deduced not only from its T_g value (-22.83 °C) but also from its ^{1}H-NMR spectrum at room temperature, which is extremely broad and poorly resolved (Figure 4.9).

These differences in viscosity were clearly visible when analyzing other transport properties, like self-diffusion and ionic conductivity. First, we will examine the self-diffusion measurements from Paper II (Figure 4.18).

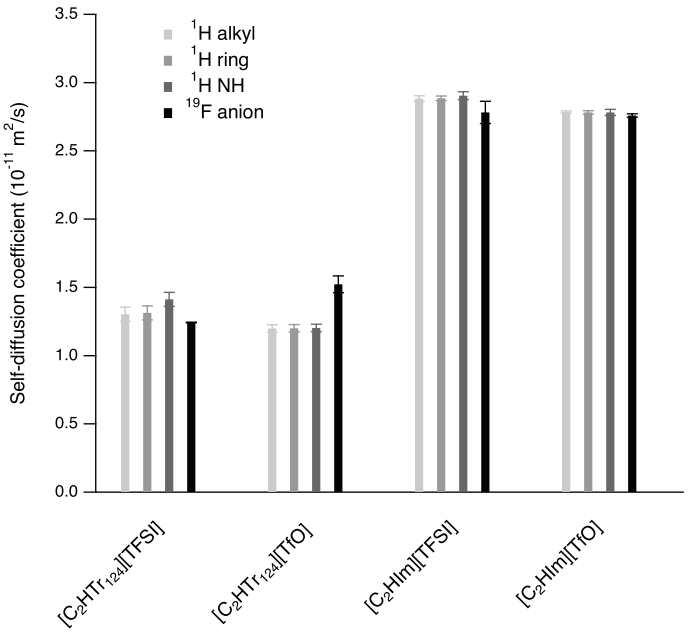

Figure 4.18: Self-diffusion coefficients estimated from PFG NMR measurements for different ^{1}H and ^{19}F resonances and for all four protic ionic liquids from Paper II at 34 °C. The errors show the standard deviation of the fitted diffusion coefficient.

The self-diffusion data for all four compounds clearly shows a distinction between the self-diffusion coefficients of triazolium- and imidazolium-based compounds, with the latter diffusing approximately twice as fast as triazolium compounds. The diffusion

experiments also indicate that the exchangeable proton (NH) diffuses primarily via the vehicular mechanism (since no significant differences in the self-diffusion coefficients of the different hydrogens were detected).[26] Interestingly, the two different anions seem to result in approximately the same self-diffusion coefficients, meaning that the cation dictates the diffusion behavior of these compounds. We speculate that once again, acidity and hydrogen bonding are responsible for these differences in self-diffusion. Since the triazolium compounds present higher acidity and stronger hydrogen bonding (Figure 4.15), they should be expected to diffuse slower compared to their imidazolium counterparts. A similar trend was found in the ionic conductivity data for these compounds (Figure 4.19).

26: If proton transport was occurring (to a significant degree) via the hopping mechanism, one should expect the self-diffusion of the NH hydrogen to be faster than the ring or alkyl group hydrogens [128].

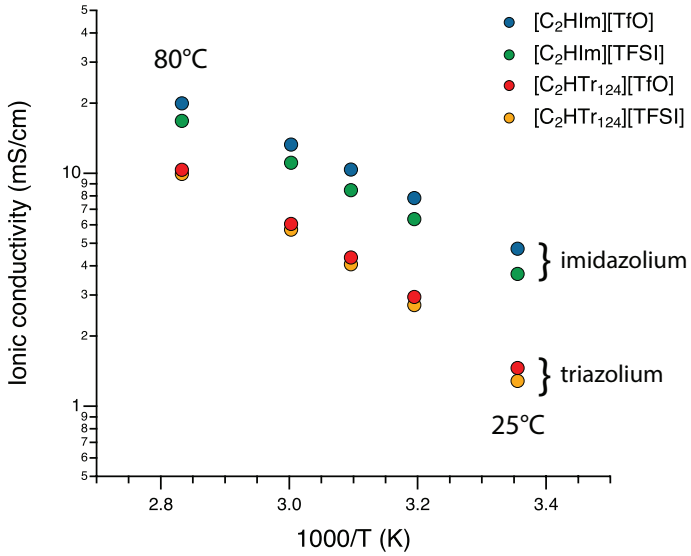

Figure 4.19: Ionic conductivity values (shown in a log scale Arrhenius plot), for all protic ionic liquids in Paper II. Measurements made in the dry and inert atmosphere of a glovebox, as a function of temperature.

The two families of compounds clearly segregate, with imidazolium-based protic ionic liquids having higher ionic conductivities, compared to their triazolium counterparts. Once again, we believe that these differences can be generally explained by the same logic used to justify the differences in self-diffusion. A similar trend was found for the compounds in Paper III (Figure 4.20). In this figure, we can see the clear difference in conductivity between all three compounds, with the two modified compounds clearly being lower in conductivity compared to the reported values for [C_4HIm][TFSI]. In fact, these two ionic liquids, ([C_4H−4-NO_2Im][TFSI] and [C_4H−4,5−$(CN)_2$Im][TFSI]), have the lowest conductivity values of any ionic liquid presented in this thesis. This is quite reasonable, since they are the most viscous (assuming that they behave as most other protic ionic liquids, without any significant proton conduction by hopping mechanisms) and likely the most acidic as well. Importantly, these conductivities follow the T_g values, meaning that the higher T_g is related to a lower ionic conductivity.

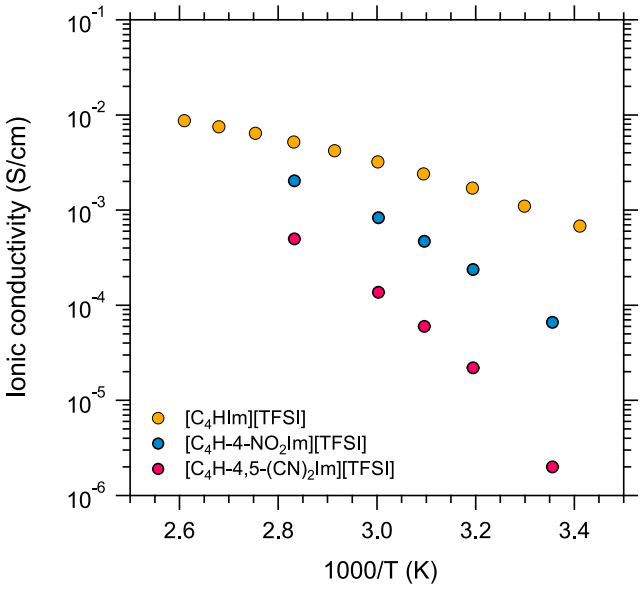

Figure 4.20: Ionic conductivity values (shown in a log scale Arrhenius plot) for all protic ionic liquids in Paper III. Measurements made in the dry and inert atmosphere of a glovebox, as a function of temperature. For $[C_4HIm][TFSI]$, original data from a previous study are reproduced [125].

As we previously discussed in the Background chapter, more information about these protic ionic liquids can be extracted from this ionic conductivity data. These plots can be scaled by using the T_g values of the ionic liquids (producing the so-called Angell plot). The result of this scaling can be seen in Figures 4.21 and 4.22.

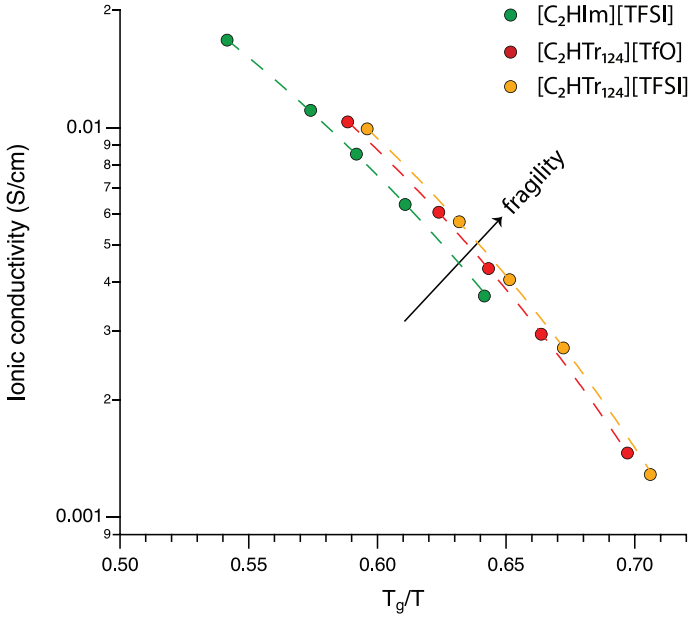

Figure 4.21: T_g-scaled conductivity plot (Angell plot) with the same experimental data shown in Figure 4.19. Note that $[C_2HIm][TfO]$ was excluded, due to a lack of T_g. Dashed lines fit to the experimental data.

The first noticeable thing in Figure 4.19 is the inversion of the conductivity curves. While in the previous Arrhenius plot, the conductivity curve of $[C_2HIm][TFSI]$ was above the triazolium compounds, now it is lower. This happens because of differences in fragility (a concept discussed in the Background chapter). If we look back at Figure 2.4 and compare it to Figure 4.19, we can see that $[C_2HIm][TFSI]$ has a behavior close to curve B, which in practice means that when we heat it from its T_g, its conductivity increases

in a slower rate compared to the triazolium compounds, therefore, it is comparably less fragile (stronger).[27] The same analysis applies to the data from Paper III (Figure 4.22).

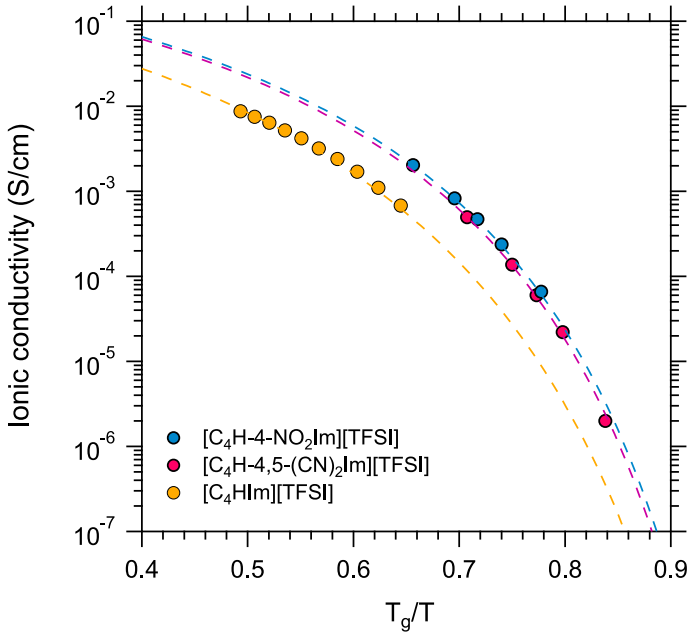

Figure 4.22: T_g-scaled conductivity plot (Angell plot) with the same experimental data shown in Figure 4.20. Dashed lines are fits to the experimental data.

In this case, [C_4HIm][TFSI] presents a significantly lower fragility when compared to its nitro- and cyano-functionalized counterparts. Overall, it appears to indicate that a higher acidity might be related to a higher fragility. The origins of fragility are still not well understood [129], but at least for protic ionic liquids based on the decahydroisoquinolinium cation [130], it appears that their fragilities are related to their ΔpK_a, which is in agreement with our findings. The origin of fragility in glass-forming liquids is certainly more complex (cannot be attributed to a single descriptor), but this data indicates that acidity (or at least its effects on the intermolecular interactions) might play an important role.

27: Fragility can also be determined quantitatively, by fitting conductivity data with the VFT equation (2.1) and estimating the D value. This was discussed in more detail in Paper II.

Conclusions and outlook 5

5.1 Summary of the main findings and results

As the title of this thesis implies, the research presented here encompasses an exploration that delves into the very basics of the synthesis of protic ionic liquids, how to analyze them, how to computationally model them, and reflections on their fundamental properties.

The work from Paper I, introduces the challenges in the synthesis of pure and dry protic ionic liquids and proposes a setup (which was further improved in Paper III) to address these challenges. With this setup, a series of protic ionic liquids could be reliably synthesized. These compounds were characterized using a range of different techniques, with a focus on properties relevant to their intended application in fuel cell systems. In order to do that without the influence of atmospheric moisture, different methodologies for sample preparation and analysis were also developed.

These analyses were further complemented by the use of molecular modeling experiments, which provided a unique perspective on how modifications to the structure of these protic ionic liquids can affect their fundamental properties. The research from Paper I demonstrated how changing the cation structure from imidazolium to triazolium has a noticeable effect on the acidity of the ionic liquid, which in turn, affects other properties. Despite their lower thermal stability, elevated glass transition temperatures, and lower ionic conductivity, triazolium-based protic ionic liquids are still quite interesting and viable alternatives to imidazolium compounds and we expect them to become more popular in the future (especially if the higher acidity is beneficial to the intended application).

In Paper III, new nitro- and cyano-functionalized protic ionic liquids were synthesized, resulting in protic ionic liquids that seem to be highly acidic, a property that might be interesting for catalytic applications where their high viscosity may be less problematic. Once again, this high acidity was correlated to lower thermal stability, higher viscosity, and lower ionic conductivity. It is important to note, that this work also provides a new strategy for developing acidic protic ionic liquids, which is quite relevant since nowadays only two strategies are commonly employed (SO_3H functionalization or the use of acidic anions). It would be interesting to explore if there are ways to modify these ionic liquids to reduce their viscosity while maintaining their higher acidity. Not only

that, but to also apply this strategy (electron-withdrawing induced increase in acidity) to other types of cations.

These conductivity measurements were made possible by the work conducted in Paper II, which describes the development of a conductivity setup that can be operated (at a range of temperatures) inside the confined and inert environment of a glovebox. The results of these ionic conductivity measurements from Paper II and III pointed to an interesting possibility, acidity (or at least the difference in ΔpK_a between the acid and the base precursors) might be correlated to fragility in protic ionic liquids. This clue might be useful in the determination of the origins of fragility in this family of compounds. Finally, the conductivity setup results still need to be validated against other techniques, such as broadband dielectric spectroscopy. Furthermore, the range of temperature at which the setup operates might be able to be extended to -40 to 150 °C, which would certainly be interesting.

5.2 Improving the synthesis of protic ionic liquids

An ongoing challenge within the field of protic ionic liquids is the discrepancy in the reported properties of supposedly identical compounds when synthesized by different research groups. While a certain level of variability is expected in any field of organic chemistry (and a certain degree of experimental error in the analysis of these properties), the one I have personally observed in the field of protic ionic liquids is in my opinion not acceptable. We must develop better ways of making these compounds. While the latest iteration of our synthesis setup (described in Paper III) is as simple as we could make it (given the constraints and challenges discussed in Paper I and III), there is still so much room for improvement. The setup is still quite expensive, since it requires a glovebox and the Polar Bear Plus system. Additionally, the synthesis procedure is still fairly complex, as can be seen in the supporting information video from Paper I. For instance, it would be interesting to see if ionic liquids of similar quality could be made outside the glovebox, by the use of Schlenk techniques. Overall, one of our hopes with Paper I is that it will serve as a starting point for a larger discussion on the synthesis of pure and dry protic ionic liquids.

5.3 Reflections on the molecular modeling of protic ionic liquids

Ionic liquids are flexible molecules. This means that even though single ion pair modeling (when well done) can still provide a lot of insight into the behavior of these molecules, it is certainly not the best representation of these systems in the bulk. Therefore, I would like to propose a few things to the community. Single-ion pair modeling should only be used if several conformers were screened at lower levels of theory (by using software like CREST for instance). It's not a perfect solution, but researchers should at least try to find a global minimum (although they will arguably never find it, at least an attempt was made to optimize the geometry as much as possible, and not simply rely on serendipity to get a low energy conformer). Furthermore, dispersion corrections should always be used. Solvation models are also highly encouraged, but more systematic studies on their effects must be conducted.

Single-ion pair studies could also potentially be improved by using conformational ensembles and calculating their properties by Boltzmann averaging according to the relative conformer energies. Certainly not trivial, since this type of modeling might require optimizing hundreds of ion pairs, depending on the molecular flexibility.

Some studies on the modeling of clusters of ionic liquids have already been conducted by the group of Prof. Ekaterina I. Izgorodina and more should be encouraged. Due to the additional degrees of freedom imposed by the modeling of clusters, this is no trivial task, but I believe that significant progress could potentially be achieved by the use of multilayer modeling schemes (e.g. ONIOM).

Regarding my own approach to extracting data from single-ion pair experiments: in my opinion, more systematic studies must be performed to validate the conclusions from this thesis regarding the acidity of protic ionic liquids. Not only that, but the dependence of the molecular descriptors (bond length, HOMO/LUMO energies, E_{HB}, etc.) on the geometry must also be further explored. For instance, in my own experience, I've noticed how HOMO/LUMO energies are quite robust to small changes in the molecular geometry, while N-H vibrational frequencies can be quite sensitive.

Although I'm quite confident about the overall computational findings of the research presented in this thesis (i.e. triazolium compounds are likely to be more acidic compared to imidazolium ones, same for nitro- and cyano-functionalized compounds), I believe that with time, as methods get better, some specific data

points presented here could be contested (a certain bond length, atomic charge, electrophilicity, etc.). Importantly, the same can be said about a large number of published studies. Still, it is important to acknowledge such limitations. These limitations should not discourage others from performing similar experiments, but should always be taken into consideration when analyzing the results.

Bibliography

(1) T. L. Greaves and C. J. Drummond, *Chemical Reviews*, 2008, **108**, 206–237 (cit. on pp. 1, 6).

(2) P. Walden, *Bulletin de l'Académie impériale des sciences de St.-Pétersbourg*, 1914, **8**, 405–422 (cit. on p. 2).

(3) M. Freemantle, *Chemical & Engineering News Archive*, 1998, **76**, 32–37 (cit. on pp. 2, 3).

(4) T. L. Greaves and C. J. Drummond, *Chemical Reviews*, 2015, **115**, 11379–11448 (cit. on pp. 2, 6, 7).

(5) W.-C. Tu, L. Weigand, M. Hummel, H. Sixta, A. Brandt-Talbot and J. P. Hallett, *Cellulose*, 2020, **27**, 4745–4761 (cit. on p. 2).

(6) P. Y. Nakasu, P. Verdía Barbará, A. E. Firth and J. P. Hallett, *Trends in Chemistry*, 2022, **4**, 175–178 (cit. on p. 2).

(7) T. Stettner and A. Balducci, *Energy Storage Materials*, 2021, **40**, 402–414 (cit. on p. 2).

(8) A. L. L. East, C. M. Nguyen and R. Hempelmann, *Frontiers in Energy Research*, 2023, **11** (cit. on pp. 2, 3, 6).

(9) H. A. Elwan, M. Mamlouk and K. Scott, *Journal of Power Sources*, 2021, **484**, 229197 (cit. on pp. 2, 6).

(10) R. Haider, Y. Wen, Z.-F. Ma, D. P. Wilkinson, L. Zhang, X. Yuan, S. Song and J. Zhang, *Chemical Society Reviews*, 2021, **50**, 1138–1187 (cit. on p. 3).

(11) K. Wippermann and C. Korte, *Current Opinion in Electrochemistry*, 2022, **32**, 100894 (cit. on pp. 3, 32).

(12) K. Wippermann, Y. Suo and C. Korte, *The Journal of Physical Chemistry C*, 2021, **125**, 4423–4435 (cit. on pp. 3, 32).

(13) H. Doi, X. Song, B. Minofar, R. Kanzaki, T. Takamuku and Y. Umebayashi, *Chemistry – A European Journal*, 2013, **19**, 11522–11526 (cit. on pp. 6, 8).

(14) W. Xu, E. I. Cooper and C. A. Angell, *The Journal of Physical Chemistry B*, 2003, **107**, 6170–6178 (cit. on pp. 6, 9, 10).

(15) B. Nuthakki, T. L. Greaves, I. Krodkiewska, A. Weerawardena, M. I. Burgar, R. J. Mulder and C. J. Drummond, *Australian Journal of Chemistry*, 2007, **60**, 21–28 (cit. on p. 6).

(16) J. Stoimenovski, E. I. Izgorodina and D. R. MacFarlane, *Physical Chemistry Chemical Physics*, 2010, **12**, 10341–10347 (cit. on p. 6).

(17) S. K. Mann, S. P. Brown and D. R. MacFarlane, *ChemPhysChem*, 2020, **21**, 1444–1454 (cit. on p. 6).

(18) M. Yoshizawa, W. Xu and C. A. Angell, *Journal of the American Chemical Society*, 2003, **125**, 15411–15419 (cit. on p. 6).

(19) M. A. B. H. Susan, A. Noda, S. Mitsushima and M. Watanabe, *Chemical Communications*, 2003, 938–939 (cit. on pp. 6, 8).

(20) D. E. Smith and D. A. Walsh, *Advanced Energy Materials*, 2019, **9**, 1900744 (cit. on pp. 6, 9).

(21) C. Y. Wong, W. Y. Wong, K. S. Loh and K. L. Lim, *Reactive and Functional Polymers*, 2022, **171**, 105160 (cit. on p. 6).

(22) H. Watanabe, N. Arai, H. Jihae, Y. Kawana and Y. Umebayashi, *Journal of Molecular Liquids*, 2022, **352**, 118705 (cit. on p. 6).

(23) N. Yaghini, V. Gómez-González, L. M. Varela and A. Martinelli, *Physical Chemistry Chemical Physics*, 2016, **18**, 23195–23206 (cit. on p. 6).

(24) M. Hasani, L. M. Varela and A. Martinelli, *The Journal of Physical Chemistry B*, 2020, **124**, 1767–1777 (cit. on p. 6).

(25) S. Zhang, J. Zhang, Y. Zhang and Y. Deng, *Chemical Reviews*, 2017, **117**, 6755–6833 (cit. on p. 7).

(26) M. P. Singh, R. K. Singh and S. Chandra, *Progress in Materials Science*, 2014, **64**, 73–120 (cit. on p. 7).

(27) R. Hayes, G. G. Warr and R. Atkin, *Chemical Reviews*, 2015, **115**, 6357–6426 (cit. on p. 7).

(28) R. Hayes, S. Imberti, G. G. Warr and R. Atkin, *Angewandte Chemie International Edition*, 2013, **52**, 4623–4627 (cit. on pp. 7, 47).

(29) D. R.MacFarlane, M. Kar and J. M. Pringle, in *Fundamentals of Ionic Liquids*, John Wiley & Sons, Ltd, 2017, ch. 5, pp. 103–147 (cit. on pp. 7, 8, 47).

(30) M. J. Earle, J. M. Esperança, M. A. Gilea, J. N. Canongia Lopes, L. P. Rebelo, J. W. Magee, K. R. Seddon and J. A. Widegren, *Nature*, 2006, **439**, 831–834 (cit. on p. 7).

(31) C. Maton, N. De Vos and C. V. Stevens, *Chemical Society Reviews*, 2013, **42**, 5963–5977 (cit. on p. 7).

(32) J. P. Leal, J. M. S. S. Esperança, M. E. Minas da Piedade, J. N. Canongia Lopes, L. P. N. Rebelo and K. R. Seddon, *The Journal of Physical Chemistry A*, 2007, **111**, 6176–6182 (cit. on p. 7).

(33) F. M. S. Ribeiro, C. F. R. A. C. Lima, I. C. M. Vaz, A. S. M. C. Rodrigues, E. Sapei, A. Melo, A. M. S. Silva and L. M. N. B. F. Santos, *Physical Chemistry Chemical Physics*, 2017, **19**, 16693–16701 (cit. on p. 7).

(34) H. Duan, F. Liu, S. Hussain, H. Dong, X. Zhang and Z. Cheng, *New Journal of Chemistry*, 2023, **47**, 11275–11284 (cit. on p. 7).

(35) C. Karlsson, C. Strietzel, H. Huang, M. Sjödin and P. Jannasch, *ACS Applied Energy Materials*, 2018, **1**, 6451–6462 (cit. on pp. 8, 31).

(36) J. Ingenmey, S. Gehrke and B. Kirchner, *ChemSusChem*, 2018, **11**, 1900–1910 (cit. on p. 8).

(37) M. Anouti, J. Jacquemin and P. Porion, *The Journal of Physical Chemistry B*, 2012, **116**, 4228–4238 (cit. on p. 8).

(38) I. Popov, Z. Zhu, A. R. Young-Gonzales, R. L. Sacci, E. Mamontov, C. Gainaru, S. J. Paddison and A. P. Sokolov, *Communications Chemistry*, 2023, **6**, 77 (cit. on p. 8).

(39) L. Wylie, M. Kéri, A. Udvardy, O. Hollóczki and B. Kirchner, *ChemSusChem*, **16**, e202300535 (cit. on p. 9).

(40) P. Sippel, P. Lunkenheimer, S. Krohns, E. Thoms and A. Loidl, *Scientific Reports*, 2015, **5**, 13922 (cit. on p. 9).

(41) R. Böhmer, K. L. Ngai, C. A. Angell and D. J. Plazek, *The Journal of Chemical Physics*, 1993, **99**, 4201–4209 (cit. on p. 10).

(42) D. R. MacFarlane, M. Forsyth, E. I. Izgorodina, A. P. Abbott, G. Annat and K. Fraser, *Physical Chemistry Chemical Physics*, 2009, **11**, 4962–4967 (cit. on p. 10).

(43) N. Yaghini, L. Nordstierna and A. Martinelli, *Physical Chemistry Chemical Physics*, 2014, **16**, 9266–9275 (cit. on pp. 10, 20).

(44) K. Damodaran, *Progress in Nuclear Magnetic Resonance Spectroscopy*, 2022, **129**, 1–27 (cit. on p. 10).

(45) A. J. Cohen, P. Mori-Sánchez and W. Yang, *Chemical Reviews*, 2012, **112**, 289–320 (cit. on p. 11).

(46) A. D. Becke, *The Journal of Chemical Physics*, 2014, **140**, 18A301 (cit. on p. 11).

(47) M. Bursch, J.-M. Mewes, A. Hansen and S. Grimme, *Angewandte Chemie*, 2022, **134** (cit. on pp. 11, 12, 28).

(48) *Introduction to Density Functional Theory (DFT) - by Prof. David Sherrill*, `https://www.youtube.com/watch?v=QGyfGCZT110`, 2020 (cit. on p. 11).

(49) L. Goerigk, A. Hansen, C. Bauer, S. Ehrlich, A. Najibi and S. Grimme, *Physical Chemistry Chemical Physics*, 2017, **19**, 32184–32215 (cit. on p. 12).

(50) J. Harvey, in *Computational Chemistry*, Oxford University Press, 2018 (cit. on pp. 12, 28).

(51) S. Koutsoukos, F. Philippi, F. Malaret and T. Welton, *Chemical Science*, 2021, **12**, 6820–6843 (cit. on p. 12).

(52) B. Kirchner, in *Ionic Liquids*, ed. B. Kirchner, Springer Berlin Heidelberg, Berlin, Heidelberg, 2010, pp. 213–262 (cit. on pp. 12, 28).

(53) E. I. Izgorodina, Z. L. Seeger, D. L. A. Scarborough and S. Y. S. Tan, *Chemical Reviews*, 2017, **117**, 6696–6754 (cit. on pp. 12, 28).

(54) S. Grimme, *Chemistry – A European Journal*, 2012, **18**, 9955–9964 (cit. on p. 13).

(55) C. M. Breneman and K. B. Wiberg, *Journal of Computational Chemistry*, 1990, **11**, 361–373 (cit. on p. 13).

(56) F. B. van Duijneveldt, J. G. C. M. van Duijneveldt-van de Rijdt and J. H. van Lenthe, *Chemical Reviews*, 1994, **94**, 1873–1885 (cit. on p. 13).

(57) P. Geerlings, F. De Proft and W. Langenaeker, *Chemical Reviews*, 2003, **103**, 1793–1874 (cit. on p. 13).

(58) P. K. Chattaraj, S. Giri and S. Duley, *Chemical Reviews*, 2011, **111**, PR43–PR75 (cit. on p. 13).

(59) K. Gupta, D. Roy, V. Subramanian and P. Chattaraj, *Journal of Molecular Structure: THEOCHEM*, 2007, **812**, 13–24 (cit. on pp. 13, 42).

(60) T. Lu and F. Chen, *Journal of Computational Chemistry*, 2012, **33**, 580–592 (cit. on pp. 14, 30).

(61) E. Espinosa, E. Molins and C. Lecomte, *Chemical Physics Letters*, 1998, **285**, 170–173 (cit. on pp. 14, 30).

(62) S. Emamian, T. Lu, H. Kruse and H. Emamian, *Journal of Computational Chemistry*, 2019, **40**, 2868–2881 (cit. on p. 14).

(63) R. F. W. Bader, *Accounts of Chemical Research*, 1985, **18**, 9–15 (cit. on pp. 14, 30, 44).

(64) B. R. Clare, P. M. Bayley, A. S. Best, M. Forsyth and D. R. MacFarlane, *Chemical Communications*, 2008, 2689–2691 (cit. on p. 15).

(65) B. Clare, A. Sirwardana and D. R. MacFarlane, in *Ionic Liquids*, ed. B. Kirchner, Springer Berlin Heidelberg, Berlin, Heidelberg, 2010, pp. 1–40 (cit. on p. 15).

(66) S. Koutsoukos, J. Becker, A. Dobre, Z. Fan, F. Othman, F. Philippi, G. J. Smith and T. Welton, *Nature Reviews Methods Primers*, 2022, **2**, 49 (cit. on p. 15).

(67) L. Cammarata, S. G. Kazarian, P. A. Salter and T. Welton, *Physical Chemistry Chemical Physics*, 2001, **3**, 5192–5200 (cit. on p. 16).

(68) D. Shriver and M. Drezdzon, *The Manipulation of Air-Sensitive Compounds*, Wiley, 1986 (cit. on p. 16).

(69) A. M. Borys, *Organometallics*, 2023, **42**, 182–196 (cit. on p. 16).

(70) Y. K. J. Bejaoui, F. Philippi, H.-G. Stammler, K. Radacki, L. Zapf, N. Schopper, K. Goloviznina, K. A. M. Maibom, R. Graf, J. A. P. Sprenger, R. Bertermann, H. Braunschweig, T. Welton, N. V. Ignat'ev and M. Finze, *Chemical Science*, 2023, **14**, 2200–2214 (cit. on p. 17).

(71) S. J. Brown, D. Yalcin, S. Pandiancherri, T. C. Le, I. Orhan, K. Hearn, Q. Han, C. J. Drummond and T. L. Greaves, *Journal of Molecular Liquids*, 2022, **367**, 120453 (cit. on p. 17).

(72) *Polar Bear Plus website*, `https://www.polarbearplus.com/polar-bear-family/polar-bear-plus/`, 2023 (cit. on p. 19).

(73) S. K. Bharti and R. Roy, *TrAC Trends in Analytical Chemistry*, 2012, **35**, 5–26 (cit. on p. 20).

(74) *MestReNova software website*, `https://mestrelab.com/`, 2023 (cit. on p. 21).

(75) P. Larkin, in *Infrared and Raman Spectroscopy*, Elsevier, 2011 (cit. on pp. 21, 40).

(76) *Original Raman scattering image from Wikipedia user Moxfyre*, `https://commons.wikimedia.org/wiki/File:Raman_energy_levels.svg`, 2023 (cit. on p. 23).

(77) M. Götz, R. Reimert, S. Bajohr, H. Schnetzer, J. Wimberg and T. J. Schubert, *Thermochimica Acta*, 2015, **600**, 82–88 (cit. on p. 24).

(78) Y. Prykhodko, A. Martin, H. Oulyadi, Y. L. Kobzar, S. Marais and K. Fatyeyeva, *Journal of Molecular Liquids*, 2022, **345**, 117782 (cit. on p. 24).

(79) C.-C. Chen and Y.-S. Huang, *Journal of Thermal Analysis and Calorimetry*, 2023, **148**, 6731–6745 (cit. on p. 24).

(80) T. D. Claridge, in *High-Resolution NMR Techniques in Organic Chemistry. Third Edition*, Elsevier, 2016 (cit. on p. 26).

(81) *How MRI works - Youtube playlist by user thePIRL*, `https://www.youtube.com/watch?v=TQegSF4ZiIQ&list=PLkSVzqeK5v2C4X1G3IuRUQeNveNGNxZrn`, 2018 (cit. on p. 26).

(82) E. O. Stejskal, *The Journal of Chemical Physics*, 2004, **43**, 3597–3603 (cit. on p. 26).

(83) Z. L. Seeger and E. I. Izgorodina, *Journal of Chemical Theory and Computation*, 2020, **16**, 6735–6753 (cit. on p. 28).

(84) C. Plett, A. Katbashev, S. Ehlert, S. Grimme and M. Bursch, *Physical Chemistry Chemical Physics*, 2023, **25**, 17860–17868 (cit. on p. 28).

(85) L. Xu, E. I. Izgorodina and M. L. Coote, *Journal of the American Chemical Society*, 2020, **142**, 12826–12833 (cit. on p. 28).

(86) L. Goerigk, A. Hansen, C. Bauer, S. Ehrlich, A. Najibi and S. Grimme, *Physical Chemistry Chemical Physics*, 2017, **19**, 32184–32215 (cit. on p. 28).

(87) M. D. Hanwell, D. E. Curtis, D. C. Lonie, T. Vandermeersch, E. Zurek and G. R. Hutchison, *Journal of Cheminformatics*, 2012, **4**, 17 (cit. on pp. 29, 30).

(88) T. A. Halgren, *Journal of Computational Chemistry*, 1996, **17**, 490–519 (cit. on p. 29).

(89) J. J. P. Stewart, *Journal of Computational Chemistry*, 1989, **10**, 209–220 (cit. on p. 29).

(90) F. Neese, *WIREs Computational Molecular Science*, 2022, **12**, e1606 (cit. on p. 29).

(91) A. D. Becke, *The Journal of Chemical Physics*, 1993, **98**, 5648–5652 (cit. on p. 29).

(92) C. Lee, W. Yang and R. G. Parr, *Physical Review B*, 1988, **37**, 785–789 (cit. on p. 29).

(93) P. J. Stephens, F. J. Devlin, C. F. Chabalowski and M. J. Frisch, *The Journal of Physical Chemistry*, 1994, **98**, 11623–11627 (cit. on p. 29).

(94) S. Grimme, J. Antony, S. Ehrlich and H. Krieg, *The Journal of Chemical Physics*, 2010, **132**, 154104 (cit. on p. 29).

(95) A. Najibi and L. Goerigk, *Journal of Chemical Theory and Computation*, 2018, **14**, 5725–5738 (cit. on p. 29).

(96) P. Pracht, F. Bohle and S. Grimme, *Physical Chemistry Chemical Physics*, 2020, **22**, 7169–7192 (cit. on p. 29).

(97) C. Bannwarth, E. Caldeweyher, S. Ehlert, A. Hansen, P. Pracht, J. Seibert, S. Spicher and S. Grimme, *WIREs Computational Molecular Science*, 2021, **11**, e1493 (cit. on p. 29).

(98) S. Grimme, A. Hansen, S. Ehlert and J.-M. Mewes, *The Journal of Chemical Physics*, 2021, **154**, 064103 (cit. on p. 29).

(99) N. Mardirossian and M. Head-Gordon, *The Journal of Chemical Physics*, 2016, **144**, 214110 (cit. on p. 29).

(100) A. V. Onufriev and D. A. Case, *Annual Review of Biophysics*, 2019, **48**, 275–296 (cit. on p. 29).

(101) V. Barone and M. Cossi, *The Journal of Physical Chemistry A*, 1998, **102**, 1995–2001 (cit. on p. 30).

(102) K. Low, S. Y. S. Tan and E. I. Izgorodina, *Frontiers in Chemistry*, 2019, **7**, DOI: 10.3389/fchem.2019.00208 (cit. on p. 30).

(103) S. Grimme, W. Hujo and B. Kirchner, *Physical Chemistry Chemical Physics*, 2012, **14**, 4875–4883 (cit. on p. 30).

(104) F. Teixeira and M. N. D. S. Cordeiro, *Journal of Chemical Theory and Computation*, 2019, **15**, 456–470 (cit. on p. 30).

(105) A.-R. Allouche, *Journal of Computational Chemistry*, 2011, **32**, 174–182 (cit. on p. 30).

(106) T. Alpers, T. W. Muesmann, O. Temme and J. Christoffers, *European Journal of Organic Chemistry*, 2018, **2018**, 4331–4337 (cit. on p. 31).

(107) E. M. Morais, I. B. Grillo, H. K. Stassen, M. Seferin and J. D. Scholten, *New Journal of Chemistry*, 2018, **42**, 10774–10783 (cit. on pp. 32, 41).

(108) S. K. Davidowski, F. Thompson, W. Huang, M. Hasani, S. A. Amin, C. A. Angell and J. L. Yarger, *The Journal of Physical Chemistry B*, 2016, **120**, 4279–4285 (cit. on p. 38).

(109) T. Cremer, C. Kolbeck, K. R. J. Lovelock, N. Paape, R. Wölfel, P. S. Schulz, P. Wasserscheid, H. Weber, J. Thar, B. Kirchner, F. Maier and H.-P. Steinrück, *Chemistry – A European Journal*, 2010, **16**, 9018–9033 (cit. on p. 38).

(110) C. Thomazeau, H. Olivier-Bourbigou, L. Magna, S. Luts and B. Gilbert, *Journal of the American Chemical Society*, 2003, **125**, 5264–5265 (cit. on p. 38).

(111) L. P. Hammett and A. J. Deyrup, *Journal of the American Chemical Society*, 1932, **54**, 2721–2739 (cit. on p. 38).

(112) H. Xing, T. Wang, Z. Zhou and Y. Dai, *Journal of Molecular Catalysis A: Chemical*, 2007, **264**, 53–59 (cit. on p. 38).

(113) Y. Geng, L. Hu, X. Zhao, H. An and Y. Wang, *Chinese Journal of Chemical Engineering*, 2009, **17**, 756–760 (cit. on p. 38).

(114) P. W. Ayers, R. G. Parr and R. G. Pearson, *The Journal of Chemical Physics*, 2006, **124**, 194107 (cit. on p. 42).

(115) A. R. Jupp, T. C. Johnstone and D. W. Stephan, *Dalton Trans.*, 2018, **47**, 7029–7035 (cit. on p. 42).

(116) D. H. Zaitsau, V. N. Emel'yanenko, P. Stange, C. Schick, S. P. Verevkin and R. Ludwig, *Angewandte Chemie International Edition*, 2016, **55**, 11682–11686 (cit. on p. 43).

(117) D. H. Zaitsau, V. N. Emel'yanenko, P. Stange, S. P. Verevkin and R. Ludwig, *Angewandte Chemie International Edition*, 2019, **58**, 8589–8592 (cit. on p. 43).

(118) W. Huang, R. Frech and R. A. Wheeler, *The Journal of Physical Chemistry*, 1994, **98**, 100–110 (cit. on p. 44).

(119) R. Arnaud, D. Benrabah and J.-Y. Sanchez, *The Journal of Physical Chemistry*, 1996, **100**, 10882–10891 (cit. on p. 44).

(120) S. P. Gejji, C. H. Suresh, K. Babu and S. R. Gadre, *The Journal of Physical Chemistry A*, 1999, **103**, 7474–7480 (cit. on p. 44).

(121) Y. Umebayashi, T. Yamaguchi, S. Fukuda, T. Mitsugi, M. Takeuchi, K. Fujii and S.-i. Ishiguro, *Analytical Sciences*, 2008, **24**, 1297–1304 (cit. on p. 44).

(122) M. S. Miran, H. Kinoshita, T. Yasuda, M. A. B. H. Susan and M. Watanabe, *Physical Chemistry Chemical Physics*, 2012, **14**, 5178–5186 (cit. on pp. 45, 46).

(123) Z. Xue, L. Qin, J. Jiang, T. Mu and G. Gao, *Physical Chemistry Chemical Physics*, 2018, **20**, 8382–8402 (cit. on pp. 45, 46).

(124) F. G. Bordwell, *Accounts of Chemical Research*, 1988, **21**, 456–463 (cit. on p. 45).

(125) I. Abdurrokhman, K. Elamin, O. Danyliv, M. Hasani, J. Swenson and A. Martinelli, *The Journal of Physical Chemistry B*, 2019, **123**, 4044–4054 (cit. on pp. 46, 47, 50).

(126) C. Xu and Z. Cheng, *Processes*, 2021, **9**, DOI: 10.3390/pr9020337 (cit. on p. 46).

(127) J. M. Slattery, C. Daguenet, P. J. Dyson, T. J. S. Schubert and I. Krossing, *Angewandte Chemie International Edition*, 2007, **46**, 5384–5388 (cit. on p. 48).

(128) N. Yaghini, I. Abdurrokhman, M. Hasani and A. Martinelli, *Physical Chemistry Chemical Physics*, 2018, **20**, 22980–22986 (cit. on p. 49).

(129) C. A. Angell and K. Ueno, *Nature*, 2009, **462**, 45–46 (cit. on p. 51).

(130) K. Ueno, Z. Zhao, M. Watanabe and C. A. Angell, *The Journal of Physical Chemistry B*, 2012, **116**, 63–70 (cit. on p. 51).